Ecosystem Services 48 (2021) 101226

Contents lists available at ScienceDirect

Ecosystem Services

journal homepage: www.elsevier.com/locate/ecoser

Piloting urban ecosystem accounting for the United States

Mehdi Heris [a], Kenneth J. Bagstad [b,*], Charles Rhodes [c], Austin Troy [a], Ariane Middel [d], Krissy G. Hopkins [e], John Matuszak [f]

[a] College of Architecture and Planning, University of Colorado Denver, Denver, CO 80202, United States
[b] U.S. Geological Survey, Geosciences & Environmental Change Science Center, Denver, CO 80225, United States
[c] U.S. Geological Survey, Science and Decisions Center, Reston, VA 20192, United States
[d] School of Arts, Media and Engineering, Arizona State University, Tempe, AZ 85281, United States
[e] U.S. Geological Survey, South Atlantic Water Science Center, Raleigh, NC 27607, United States
[f] National Council on Science and the Environment, Washington, DC 20005, United States

ARTICLE INFO

Keywords:
Experimental ecosystem accounting
System of environmental-economic accounting
Urban ecosystem services
Urban heat mitigation
Rainfall interception
Urban trees

ABSTRACT

In this study, we develop urban ecosystem accounts in the U.S., using the System of Environmental-Economic Accounting Experimental Ecosystem Accounting (SEEA EEA) framework. Most ecosystem accounts focus on regional and national scales, which are appropriate for many ecosystem services. However, ecosystems provide substantial services in cities, improving quality of life and contributing to resiliency for substantial parts of the population. Our models estimate energy savings for indoor cooling resulting from heat mitigated by trees and rainfall intercepted by trees. Both models cover major cities in the contiguous U.S. and report the results through physical supply and use tables for multiple accounting periods (2011 and 2016). Using conservative assumptions, urban trees provide substantial heat mitigation (4,098 and 4,229 GWh, valued at $523 and $539 million in 2011 and 2016, respectively) and rainfall interception (2,422 and 2,627 million m^3, valued at $434 and $425 million for 2011 and 2016, respectively). Interannual differences largely reflect variations in weather patterns. Our work shows how Earth observation data can support urban ecosystem accounting. We provide model code within a public repository to facilitate model runs elsewhere, enabling the SEEA EEA and Earth observation user communities to reuse our models and provide feedback for improvement.

1. Introduction

Natural capital accounting extends conventional economic measures to more transparently show the environment's role in supporting economic activity (Boyd et al., 2018). In both public- and private-sector settings, natural capital accounting seeks to integrate environmental accounts with conventional economic measures that previously ignored environmental contributions or attributed all environmental contributions to economic actors. For example, the value generated by growth of a stand of trees has typically been attributed to the owner of forest land, and none to environmental processes that contribute to tree growth without direct human cultivation (Obst et al., 2016). Natural capital accounting may include accounts for minerals, natural resources, or contributions to people from complex ecological processes that may not be easily measured—for example, outdoor environments for a variety of recreation activities, or the ability of a locale to convey heavy rains without inundating homes or businesses.

National statistical agencies have refined accounting frameworks over the past decades to record economic transactions at national and subnational scales, including inputs from the natural environment and those from economic inputs including labor, manufactured capital, intermediate economic goods, and from outside national borders. A nation's gross domestic product is a broad indicator of economic activity from these efforts. Researchers and agencies compile national data in many dimensions, across industries, and methodologically using statistical techniques and approximations, using the System of National Accounts.

The System of National Accounts is an international statistical system, which by using common definitions and measures enables comparison of accounts data across nations. In recent years, the United Nations has led development of international standards for environmental accounting, the first of which, the System of Environmental-Economic Accounting Central Framework (SEEA CF), was officially adopted in 2012 (United Nations et al., 2014a). The SEEA CF provides

* Corresponding author.
E-mail address: kjbagstad@usgs.gov (K.J. Bagstad).

https://doi.org/10.1016/j.ecoser.2020.101226
Received 18 June 2019; Accepted 10 November 2020
2212-0416/Published by Elsevier B.V.

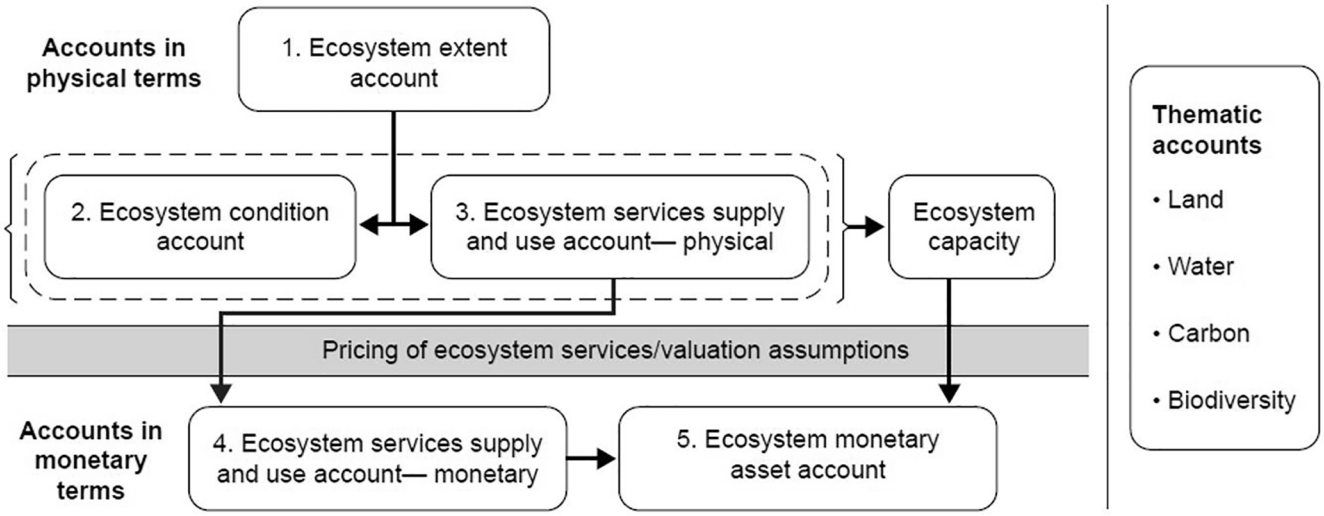

Fig. 1. Components of ecosystem accounts (adapted from United Nations, 2017).

accounting standards for natural assets and inputs to economic production, including timber, fish, water, and energy assets. The SEEA Experimental Ecosystem Accounting (SEEA EEA) framework extends the SEEA CF to include amounts of the stocks of ecosystem assets and the flows of services they deliver to the economy and society (United Nations et al, 2014b; United Nations, 2017). As with the System of National Accounts and SEEA CF, the SEEA EEA accommodates many types of accounts, including core accounts plus others serving supportive or experimental functions (see section 1.1).

Accounting perspectives such as SEEA EEA that treat ecosystem services as transactions between an ecosystem unit and an economic unit must by definition address urban ecosystems. Urban ecosystems, as any other type of ecosystem, produce a variety of ecosystem services (Keeler et al., 2019). Some cities may appear to be less ecologically diverse or productive than "natural" ecosystems such as forests or wetlands. However, larger human populations interact more frequently with urban ecosystems, increasing the number of physical transactions and typically the value for urban ecosystem services (Elmqvist et al., 2015; McPhearson et al., 2015). Urban ecosystems can also provide different types of services than non-urban systems. A falcon in a remote area that no person sees may not enter ecosystem accounts as an ecosystem service, but a falcon in an urban area should be counted as an ecological product of the urban ecosystem that may be valued by many city dwellers. In some places, even a small number of trees can provide ecosystem services that affect well-being for city residents (Wolch et al., 2014). Urban ecosystem accounting provides a framework for quantifying the extent and condition of urban ecosystems and the services they provide and associating these services with beneficiaries. Ecosystem accounting is not yet commonly used by local city planning institutions. However, the planning practice can benefit from standardized frameworks to track trends in the provision and use of important urban ecosystem services and their environmental justice impacts (Riley & Gardiner, 2020). Such reporting can, for instance, be useful for tracking the goals of city climate-action plans. This study shows how the SEEA EEA framework may be used in urban contexts to support planning.

In the growing field of natural capital accounting, a deep literature on urban ecosystem accounting has yet to emerge. Work in Canada (Grenier, Lantz, Soulard, & Wang, 2020; Statistics Canada, 2016), the United Kingdom (Anderson, 2018), and Norway (NINA, 2019) are among the first to attempt a rigorous analytic foundation, though a large body of research on urban ecosystem services can provide a basis for urban ecosystem accounts (Keeler et al., 2019). Specifically, U.K. urban ecosystem accounts quantify natural land cover, functional green space, publicly accessible green space, and blue spaces in urban-area-specific ecosystem accounts (Anderson, 2018). The extent, condition, and accessibility of different types of green space in the U.K. are tracked. The U.K. accounts also assess the ecosystem services of urban woodland environments including carbon sequestration, air filtration, cooling impact, and noise mitigation. Although the most comprehensive urban ecosystem accounts to date, U.K. work remains both experimental and partial. With the exception of accounts for visitation to urban green space and property value premiums from open-space proximity, U.K. ecosystem accounts are for a single year. Ecosystem accounts in Canada have quantified changes in ecosystem extent, i.e., land cover, noting particularly the conversion of forests, shrublands, and agricultural land to urban land uses (Grenier et al., 2020; Statistics Canada, 2016). Additionally, experimental work is underway to develop urban ecosystem accounts for Norway (NINA, 2019). Urban trees provide critical benefits where a significant part of the population lives; in the U.S., about 40% of the population lives in cities with a population of 50,000 or more (Cohen et al., 2015). Recent nationwide declines in urban tree canopy cover and increases in impervious surfaces have strong implications for the delivery of urban ecosystem services (Nowak & Greenfield, 2018). This shows the importance of urban ecosystem accounts for the U.S. that are compiled at the national scale but provide first-estimate city-level data about the value that urban trees provide and the consequences of their loss. Urban ecosystem accounts can provide information useful for community and city-level planning, as well as informing national-scale progress, for example, on Sustainable Development Goal 11, Sustainable cities and communities (United Nations, 2015).

In developing urban ecosystem accounts for the U.S., extensive literature shows that connection to nature in urban areas—specifically vegetation and trees—benefits physical and mental health (Beatley, 2011; Bratman et al., 2019). Trees mitigate urban heat (Aminipouri et al., 2019; Kong et al., 2016; Livesley et al., 2016; Middel et al., 2015; Mullaney et al., 2015; Willis & Petrokofsky, 2017), stormwater runoff (Klingberg et al., 2017; McPherson et al., 2011), noise (Klingberg et al., 2017), and air pollution (Nowak et al., 2006; 2014). Numerous studies have quantified the mechanisms through which trees benefit people living in built environments. Such studies most often use intensive experiments in small areas. The challenge of accounting for urban ecosystem services at national scales is that the required data and models are often not available for entire cities, and relationships underlying ecosystem service provision may vary by city, i.e., depending on its size, density, or climate zone (Keeler et al., 2019; Steele & Wolz, 2019).

1.1. Ecosystem accounting framework

The SEEA EEA provides the standard structure for a series of tables that quantify attributes of ecosystems and the services they provide to people, in a manner theoretically compatible with the System of National Accounts and SEEA CF (United Nations et al., 2014b; United Nations, 2017; Fig. 1). Since the accounts are inherently spatial, their outputs are often presented as maps as well as tables. Ecosystem extent accounts (1) measure changes over time in the area of different ecosystem types (see below), while ecosystem condition accounts (2) measure various attributes of ecosystems, particularly those relevant to their ability to produce the biophysical elements created by ecosystem processes (ecological end-products) that are used in ecosystem services now and into the future (Warnell et al., 2020). Ecosystem extent and condition typically influence the physical supply of ecosystem services (3), which are either directly measured or biophysically modeled in tandem with data on their use. A variety of valuation approaches (Obst et al., 2016) can provide monetary values of ecosystem service flows (4) or the net present value of stocks of ecosystem assets (5). Thematic accounts organize additional information on natural capital topics including land (Wentland et al., 2020), water (Bagstad et al., 2020), and carbon and biodiversity (Warnell et al., 2020). Data from thematic accounts can aid in the compilation of other ecosystem accounts, be used in standalone analysis, or support wider analysis of ecosystem accounting information (United Nations, 2017). Finally, capacity accounts quantify ecosystems' potential to supply ecological end-products now and into the future, whose volume may differ from the quantity of services actually used by people (Hein et al., 2016).

Because of the spatial nature of ecosystem services, ecosystem accounts must quantify how ecosystems, their characteristics, and their services are distributed on the landscape. SEEA EEA thus also specifies a set of spatial units for ecosystem accounting. A first premise of SEEA EEA is that complex functioning ecosystems are spatially separable, and that in parallel to economic production, each of the ecosystem types[1] that together compose an ecosystem accounting area (EAA)[2] produce flows of ecosystem services to economic units (i.e., specific industries, households, and governments, plus imports and exports). An ecosystem service flow is then a transaction between a place (an ecosystem asset) and a person or institution (economic unit), just as supply and use tables depict flows of goods and services from manufacturers to purchasers (United Nations, 2017). Spatial separation of "ecosystem assets" for accounting purposes does not presume that ecosystem units are ecologically independent, but simply separates where the economic transaction (human uptake of the ecosystem service) occurs within the EAA, or where a specific ecological process is measured in ecosystem condition, capacity, or thematic accounts. Ecosystem services are spatially explicit, with well-defined ecological end-products and human users (e.g., where a stretch of river through a developed area floods or not); the ecosystem types enable their attribution by specific ecosystems. In addition to EAAs and ecosystem types, United Nations, (2017) specifies basic spatial units as the smallest level of analysis in ecosystem accounting. Basic spatial units are usually summarized by grid cells. Many urban ecosystem services are "produced" by trees, and ecosystem types occur at a coarser scale than basic spatial units. An individual cell that contains some trees might be part of a forest or an urban open-space ecosystem type. The use of grid cells as a basic spatial unit enables the models to aggregate ecosystem services across ecosystem types.

To build initial urban ecosystem accounts for the U.S., we modeled heat mitigation and rainfall interception by trees in cities. Both are important urban ecosystem services, as described below.

1.2. Heat mitigation impact of trees

Trees mitigate urban heat primarily through two processes. First, they intercept direct sunlight and cast shade on buildings and surrounding ground surfaces, thereby reducing mean radiant temperature (the amount of heat that is received through radiation and is a measure of thermal comfort) at the pedestrian level, deceasing urban surface temperatures, and lowering cooling energy use of buildings (Gillner et al., 2015; Kong et al., 2016; Shashua-Bar & Hoffman, 2000; U.S. Environmental Protection Agency, 2014). Second, trees reduce air temperature through evapotranspiration (Oke, 1989). Both effects vary by climatic region, season, time of day, and tree species. Middel et al. (2015) modeled various tree planting scenarios under current and future climate for a residential neighborhood in Phoenix, AZ, and found an average air temperature reduction of 0.14 °C per 1% tree canopy increase across all scenarios. In a somewhat less arid climate, Heris et al. (2020a) found that trees reduce afternoon mean radiant temperature by 10–15 °C in two neighborhoods in Denver and Boulder, CO, while lowering air temperature by less than 1 °C at an ambient range of 25–30 °C. Ziter et al. (2019) similarly found the impact of trees on reducing site-scale air temperature to be less than 1 °C in Madison, WI. Aminipouri et al. (2019) modeled the impact of street trees on pedestrian thermal comfort and yielded an average mean radiant temperature cooling benefit of 2.1–4.2 °C across Vancouver's local climate zone. Middel & Krayenhoff (2019), in an observational study, found a peak mean radiant temperature difference of 33.4 °C between a tree-shaded location and a sun-exposed asphalt parking lot, an above-ground air temperature difference of 1.6 °C, and a surface temperature difference of 20 °C. Tan et al. (2016) observed that trees create better daytime thermal comfort by reducing mean radiant temperature in high-density urban areas, as they lower sky view factor (the extent of the sky that is observed; less sky exposure means that less direct and indirect energy is received). They conclude that tree plantings that account for wind direction and intensity can best contribute to heat mitigation. Mackey et al. (2017) argue that wind, direct short-wave radiation, and surface temperature are the most important factors in site-scale microclimate modeling; trees affect all of these variables.

In a comprehensive review of the literature regarding the impact of urban heat on energy consumption, Santamouris et al. (2015) summarized 15 studies from around the world (including eight from the U.S.). They reported that for every 1 °C increase in air temperature, energy consumption increases between 0.5% and 8.5%. The underlying studies used various methods and metrics (i.e., daily vs. monthly energy consumption) and report a relatively wide range of the impacts of urban heat on energy use. While recognizing the importance of regional variability in the relationship between heat and energy use as a function of climatic and cultural factors, regional variability is still relatively poorly understood and requires more systematic evaluation.

Given that the urban heat island effect is known to raise temperatures 2–4 °C (Deilami et al., 2018), the impact on energy use can be considerable. Akbari et al. (2001) estimated that the electricity demand for cooling buildings increases by 5–10% to compensate for the urban heat island effect in Los Angeles. Some studies have aggregated such impacts across the country and provided monetized values. For example, Nowak et al. (2017) and McDonald et al. (2020) estimate national residential cooling energy savings provided by trees at $4.7 billion and $1.0–1.6 billion, respectively.

[1] Ecosystem types are homogeneous areas of, for example, forests, wetlands, or croplands, whose configuration can change over time (United Nations, 2017). While land cover types cannot fully characterize ecosystems, in practice, land cover is often used as a proxy for ecosystem types in ecosystem accounts (Warnell et al., 2020). Ecosystem condition and supply and use tables quantify relevant ecosystem characteristics or production of ecosystem services, respectively, by ecosystem type.

[2] An ecosystem accounting area can be a political or physical boundary of management interest (e.g., watershed, biome) across which values for ecosystem accounts are summed (United Nations, 2017).

1.3. Rainfall interception by trees

Trees slow the movement of water through the hydrologic cycle, intercepting rain and storing water, which affects the volume and timing of runoff. The proportion of intercepted water compared to throughfall (water that is not intercepted) is small yet meaningful at urban scales. Rainfall interception reduces the velocity and quantity of runoff and surface pollutant wash-off (Xiao & McPherson, 2002). This ultimately reduces stormwater treatment costs. Interception is a function of (1) the intensity and duration of storm events; (2) microclimate parameters such as temperature, relative humidity, wind, and pressure; (3) tree structure such as branch shape and size; and (4) leaf area and density (leaf area index) (Stovin et al., 2008; Xiao et al., 2000). Trees most effectively intercept rainfall during small storm events (Stovin et al., 2008), so they may not substantially influence flood mitigation during extreme events. However, trees store rainfall and release water gradually. This process can increase the effectiveness of water absorption by permeable surfaces around trees, reducing runoff. Klaassen et al. (1998) modeled the amount of interception that evaporates and found that up to 30% of the intercepted water can be evaporated, depending on the climatic variables, while the remaining water gradually drips to the surface.

Reducing stormwater runoff by trees has multiple benefits. First, without trees, larger peak flows would require higher-capacity infrastructure. In cities with separate stormwater sewers, increased peak flows can lead to streambank erosion. In cities with combined sewer outfall (CSO) systems, where stormwater runoff and sanitary sewage share the same pipe, increased stormwater flows result in higher treatment costs at the wastewater treatment plant and combined sewer overflows to waterways.

Xiao and McPherson (2002) estimated that urban trees intercept about 193,000 m^3 (6.6 m^3 per tree) per year in Santa Monica, CA, potentially saving about $110,000 in stormwater treatment costs. The Center for Urban Forest Research (2002) estimated that rainfall interception by a medium-sized tree can reach up to 65 gallons per year in Sacramento, CA. However, these numbers vary greatly based on the length and intensity of different storm events, climatic region, and by tree species. Xiao et al. (1998) quantified interception in Sacramento and found that annual interception was about 11% during the leaf-on season and about 1% during the leaf-off season. Within the Blue River watershed in Kansas City, MO, the urban tree canopy intercepted 3.3% of total precipitation falling in the city while short vegetation intercepted an additional 1.4% (Nowak et al., 2013).

Narayanan & Pitt (2002) found that the capital cost of contaminant removals (mostly floatable debris and oil removal from stormwater runoff from impervious surfaces) can vary between $2,000 to $4,000 per acre per year. Other stormwater best-management practices can provide similar benefits in the absence of or together with trees. For example, the construction cost of a rain garden is about $10-$20 per square foot (Costhelper, 2019); maintenance is a considerable portion of its lifecycle cost. As a rule of thumb, Erickson et al. (2010; P:81) suggest that the cost of maintaining stormwater treatment initiatives "will roughly equal the construction cost after 12 years for a $10,000 installation and 25 years for a $100,000 installation." In summary, trees provide a considerable savings in stormwater treatment through rainfall interception.

In this study, we focus on urban trees as critical providers of heat and stormwater mitigation. While this is an admittedly limited list of ecosystem services compared to the U.K.'s more comprehensive urban ecosystem accounts, our work covers a larger geographical area and provides pilot results for the U.S. that can be expanded in future work to cover more ecosystem services. For instance, the air-quality benefits provided by trees have been recently calculated in subnational ecosystem accounts for the U.S. Southeast (Warnell et al., 2020). Our initial models include estimation of the physical and monetary supply and use of (1) energy savings for indoor cooling as a result of heat mitigated by trees and (2) rainfall intercepted by trees. Both models cover the contiguous U.S. at 30-meter resolution for the years 2011 and 2016, and aggregate physical supply and use accounts for urban areas (accounts can be flexibly aggregated; for instance, rainfall interception can also be estimated at the watershed scale). Our work supports a larger U.S. SEEA accounting effort (Bagstad et al., 2020; Boyd et al., 2018; Warnell et al., 2020; Wentland et al., 2020) as well as ongoing efforts to develop ecosystem accounts in urban areas where ecosystem services are generated through complex interactions between built and natural environments (Keeler et al., 2019).

2. Methods

We developed our models to be flexible and reusable for ecosystem accounting, enabling the automated aggregation of results to any polygon layer as the EAA. The EAAs that we used in this study include (1) municipal boundaries extracted from Census Places (U.S. Census Bureau, 2019) including municipalities and Census Designated Places with a population of 50,000 or more (n = 768); and (2) watershed boundaries, which we used to provide an aggregation example for rainfall interception in Denver, CO, at the 10-digit Hydrologic Unit Code (HUC 10) level (U.S. Geological Survey, 2017). While we could have used larger metropolitan statistical areas as EAAs, these include suburban, exurban, and rural counties adjacent to cities where ecosystems providing heat mitigation and rainfall interception are less likely to be scarce, hence less valuable, than in denser core urban areas. All EAAs used in this study are for the contiguous U.S. We classified ecosystem types based on land-cover types provided by the National Land Cover Database (NLCD, Yang et al., 2018). Other applications of the SEEA EEA have frequently used land cover as a proxy for ecosystem types (e.g., Warnell et al., 2020). The analysis and basic spatial unit of our models is 30-meter cells with the same alignment as the NLCD data. We used these data to compile physical and monetary supply and use tables for both heat mitigation and rainfall interception for the years 2011 and 2016.

2.1. Data sources

a. NLCD tree canopy, land cover, and impervious surface layers: We used 2011 and 2016 NLCD data for percent tree canopy cover, percent impervious surface, and land cover (Yang et al., 2018)[3]. We used the most recent versions of these data, published in 2019. Since the same algorithm is used for producing 2011 and 2016 data, we were able to compare the results of our models for both years. This dataset does not cover parts of Arizona (notably the cities of Avondale, Buckeye, Goodyear, and Yuma, AZ) due to problems detecting tree canopy cover in a small number of Landsat scenes.

b. Surface temperature layer: We produced a summer (June, July, and August) daytime surface temperature raster layer from Landsat 8 images for the contiguous U.S. (Fig. 2). To produce a national surface temperature layer, we downloaded four summer images for each Landsat scene with the least cloud cover for years 2013–2018. We calculated surface temperature using thermal band 10 of Landsat 8, based on USGS guidelines (U.S. Geological Survey, 2019). The Landsat scenes have overlap on each edge. Since we downloaded four images per scene, some overlapping areas can include data from up to 16 images. In order to minimize the edge effect and surface temperature disparities, we used the median value for overlapping pixels.

c. Climate data: For weather station-level data such as air temperature and precipitation, we downloaded daily summaries for each year (2011, 2016) from the Climate Data Online website (Menne et al., 2012). This dataset provides daily maximum and minimum temperature and precipitation data (National Centers for Environmental Information,

[3] While a NLCD tree canopy dataset was produced for 2001, it used different definitions for trees and different methodology (Greenfield et al., 2009) and therefore is not suitable for time series analysis and ecosystem accounting.

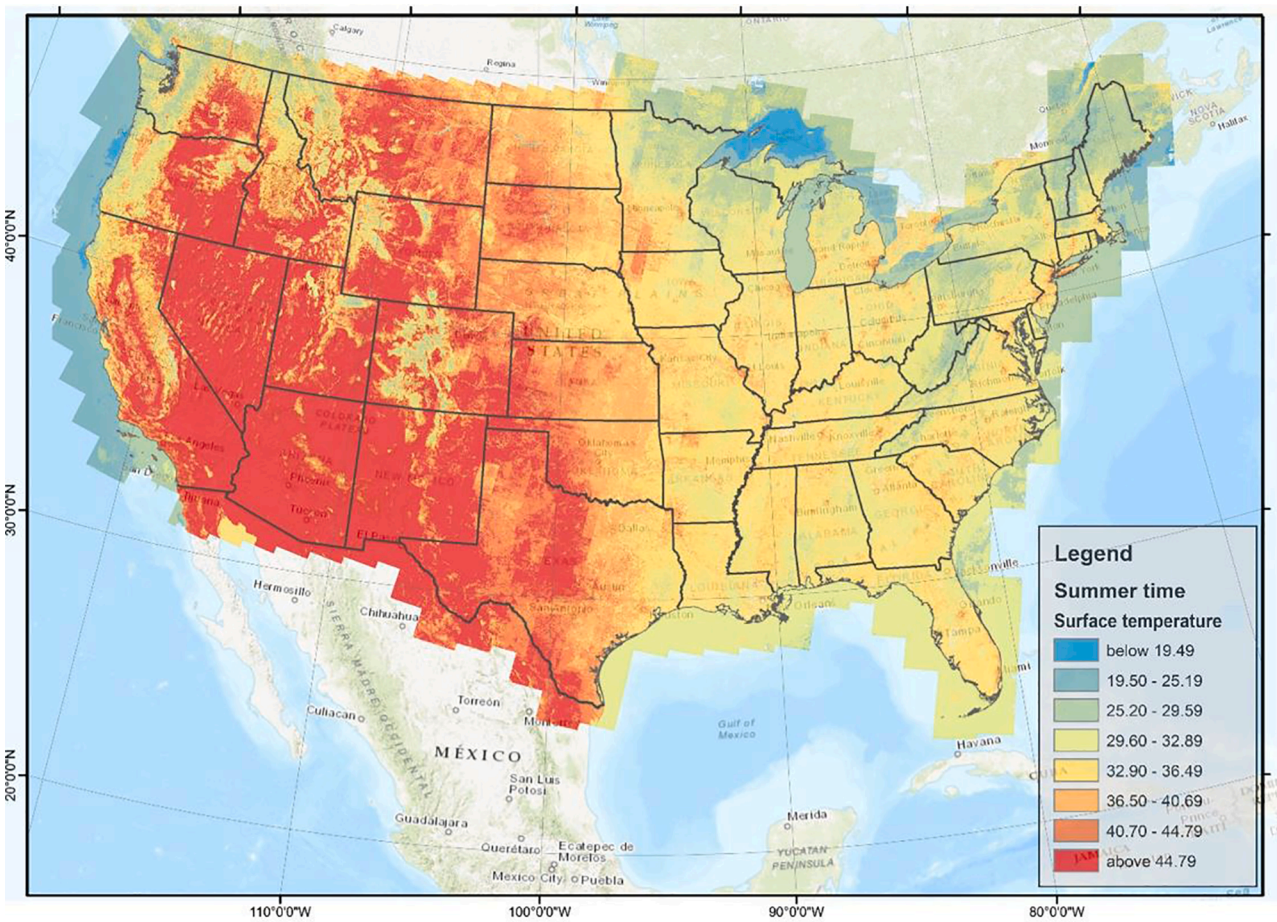

Fig. 2. Summer, daytime surface temperature from Landsat 8 thermal band data.

2018). We extracted all stations in the contiguous U.S. (n = 58,117). We used the temperature data in the heat mitigation model and precipitation data for the rainfall interception model.

d. Leaf Area Index (LAI): For the rainfall interception model, we used LAI raster data provided by the Copernicus Global Land Service (Copernicus Global Land Service, 2020). These data became available starting in 2014, so we used data for one year (2015) for both the 2011 and 2016 interception modeling. These data are a 10-day product with global coverage and 300 m resolution. For leaf-off time, we chose a 10-day period in January (10th-20th) and for leaf-on time, we chose a 10-day period in August (10th–20th).

e. Moderate Resolution Imaging Spectroradiometer (MODIS) phenology data: To assign leaf-on and leaf-off time for the rainfall interception model, we used phenology data for the start and end of the growing season extracted from MODIS images. These data are available through the MODIS Vegetation Monitoring project at 250 m resolution (Meier & Brown, 2014).

f. Average energy use for residential buildings: To connect the cooling impact of trees to energy-use reductions, we used the Building Energy Performance Database developed and maintained by the U.S. Department of Energy (2019). We extracted generalized energy-related characteristics of residential buildings by U.S. state. This database provides detailed energy use intensity data on other building types (i.e., commercial, industrial, institutional) and cooling systems as well. However, since we do not have detailed, spatial nationwide building-type data, we used the average residential building energy use intensity by state KBTU/ft^2/year (Kilo British Thermal Unit per square foot per year).

g. Land use: We used the National Land Use Dataset (Theobald, 2014) to assign industries and households benefiting from heat mitigation by North American Industry Classification System (NAICS) class (U.S. Office of Management and Budget, 2017) in the physical use table. Land-use classes in the National Land Use Dataset can be assigned corresponding NAICS classes for use in SEEA CF and EEA accounting (Warnell et al., 2020).

h. Buildings data: We used a rasterized version of the national building dataset generated by Microsoft (Microsoft, 2018) to provide total building footprint for each 30-m cell (Heris et al., 2020b). We used this layer in the heat mitigation model to associate cooling impacts with building footprint areas.

i. Combined Sewer Overflow Systems (CSO): We used the EPA Enforcement and Compliance History Online (ECHO) database to identify cities with combined sewer systems (U.S. Environmental Protection Agency, 2020). Cities with combined sewer systems tend to be older cities and small communities located in the Northeast, Midwest, or Northwest. Among 768 cities (with population of 50 k and above), 130 cities (17%) have a combined sewer system that serves part of the city.

2.2. Heat mitigation model

To estimate the energy-saving impacts of urban trees, we used a four-step approach (Fig. 3). We first developed a linear regression model to estimate surface temperature (dependent variable) as a function of NLCD tree cover and impervious surface cover (independent variables) to estimate the impact of trees on surface temperature reduction. Next, we used weather station data to build a second regression model that estimates maximum air temperature (dependent variable) as a function of surface temperature, building footprint area, and latitude

(independent variables). In the third step, we coupled these two models to estimate the impact of trees on air temperature. We used the error propagation method from Taylor (1997) to calculate the accumulated prediction uncertainties. Finally, we used building footprint area, building energy performance data, and the output of the air-temperature models to estimate the cooling energy savings provided by trees. We used the average energy cost for each state to monetize the value of energy savings provided by urban trees. To report the results at EAA level in supply and use tables, we aggregated the cell-based energy saving values using municipal boundaries.

Step 1: We first built an independent bivariate regression model of surface temperature for every city as a function of cell-level tree and impervious surface cover–predictors that have been widely used in urban heat island modeling (Deilami et al., 2018). Building individual models for each city allows us to incorporate local disparities in the relationship between tree cover, impervious surface cover, and surface temperature. We kept the models simple (instead of using more sophisticated models such as decision trees or random forests) since each model needs to be scrutinized for multicollinearity, overfitting, and other regression diagnostics. The number of cells is large enough that the regression results are statistically significant. The smallest city contains 5,208 cells, and the average number of cells for all cities is 368,450. To keep the algorithm efficient, we converted the raster data (cells) to Numpy arrays.

We tested the models for multicollinearity and statistical significance of the coefficients (alpha = 0.025). In testing the addition of other variables such as land cover and ecoregions, we did not observe a significant improvement in the quality of models while multicollinearity often became problematic when we added additional independent variables.

The relationship between tree cover and surface temperature was positive in 32 out of 768 cities, and we excluded these cities from our accounting tables. The median R^2 values for the remaining 736 cities was 0.39 and 0.40 for 2011 and 2016, respectively. Variables such as city size or location did not indicate low R^2 values. However, most major cities have relatively strong R^2 values (over 0.45) (SI Table 1 reports R^2 and regression model coefficients for each city). The only trend we observed was that cities with warm/hot and arid climate such as Phoenix, AZ, Las Vegas, NV, and San Diego, CA, had low R^2 values ($R^2 \leq 0.11$).

Step 2: Since we lack high-resolution and nationwide observed air temperature data, we built a nationwide model that estimates air temperature (dependent variable) based on surface temperature, total building footprint area, and latitude (independent variables). The existing nationwide PRISM air temperature data are both coarse resolution and highly correlated with elevation due to their estimation methods (Daly et al., 2008). The relationships between local-scale surface temperature and observed air temperature at weather stations showed good correlations, which indicated that this relationship could be used to estimate first-order effects. To more reliably estimate ambient temperature, we downloaded daily summary data from U.S. weather stations. We used 8,000 stations with daily temperature readings, for which we calculated average summertime maximum and minimum temperature (June 15th to August 15th). For each station, we extracted the average surface temperature of its neighborhood (1,000-m radius). We then built the above-described regression model. SI Table 2 shows

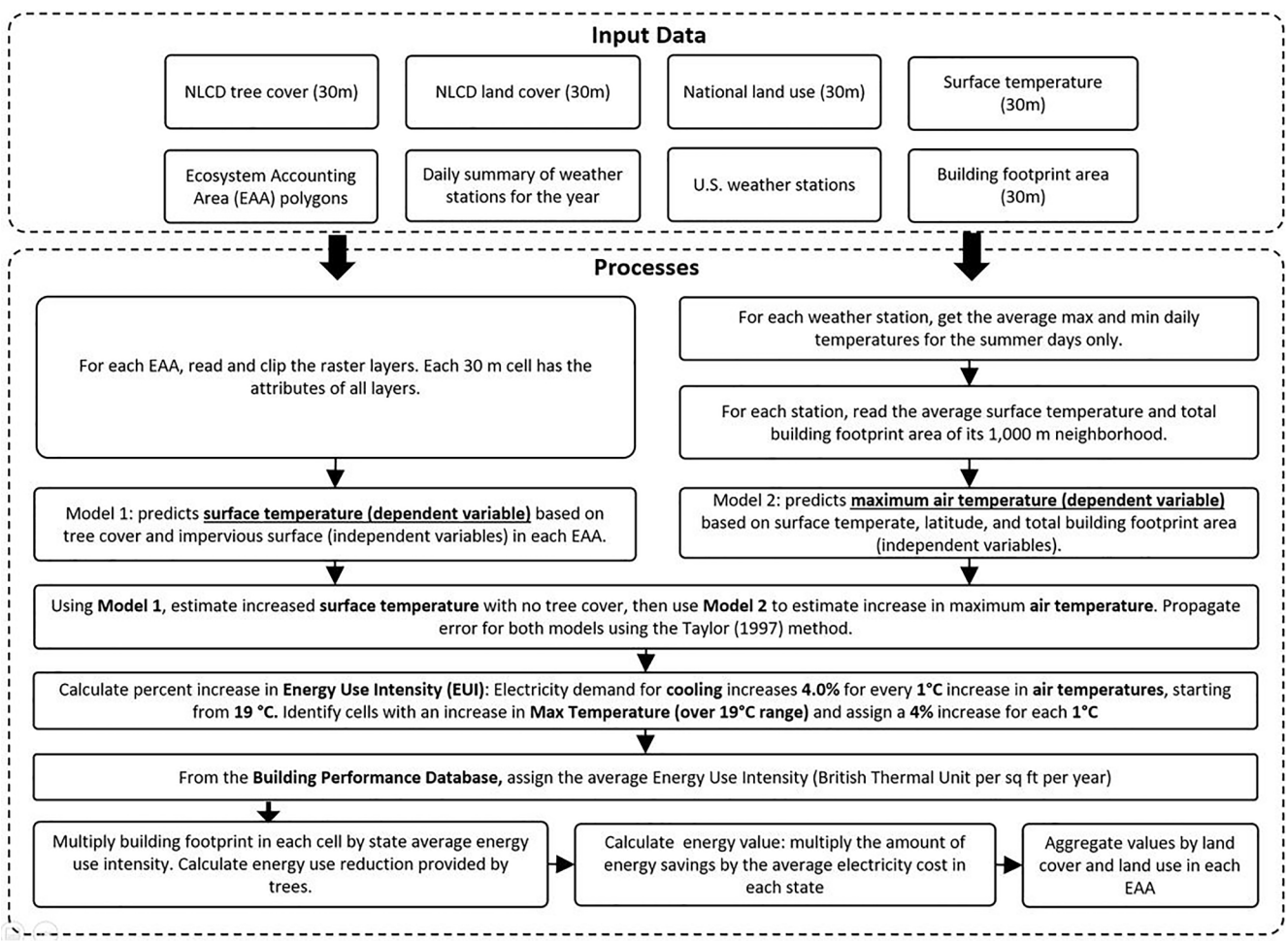

Fig. 3. Algorithm to estimate energy savings from the cooling impact of trees.

the regression model summary.

Step 3: In this step, we coupled both models to build a zero-tree scenario. First, we assigned a value of zero to tree cover and estimated surface temperature in the absence of trees for each city. Then, we used the second model and estimated air temperature for the zero-tree scenario, based on estimated surface temperature for the zero-tree scenario. We subtracted actual estimated air temperature from estimated air temperature for the zero-tree scenario to quantify the cooling impact attributable to trees. Since we combine two models, the uncertainty of both models needs to be taken into account. To propagate error, we used the Taylor (1997) method, which is also used by McDonald et al. (2020). For each prediction, we took the observed upper and lower confidence interval (alpha = 0.05) values from cell-level predictions and calculated the fractional error of each model (Frost, 2017). Finally, we used Eq. (1) to calculate the fractional uncertainty of the cooling impact of urban trees:

$$FractionalUncertainityofcoolingimpactsoftrees = \sqrt{\left(\frac{\delta_{ea}}{|ea_{best}|}\right)^2 + \left(\frac{\delta_{es}}{|es_{best}|}\right)^2 + \left(\frac{\delta_{eat0}}{|eat0_{best}|}\right)^2 + \left(\frac{\delta_{est0}}{|est0_{best}|}\right)^2} \quad (1)$$

where δ is error, *ea* is estimated air temperature, *es* is estimated surface temperature, *eat0* is the estimated air temperature for the zero-tree scenario, and *est0* is the estimated surface temperature for zero-trees scenario.

Step 4: Finally, we estimated the energy savings associated with tree cooling impacts in four steps. First, we used the Building Energy Performance Database (U.S. Department of Energy, 2019) to retrieve the average energy use intensity of residential buildings in each state. We built on a review by Santamouris et al. (2015) to quantify electricity savings, assuming that for every 1 °C increase in temperature (above 19 °C as the inflection threshold), electricity use increases by 4%, which is the middle of the range (0.5% to 8.5%) reported by Santamouris et al. (2015). Lacking a systematic understanding of regional variability in energy savings, we applied this value nationwide. Second, for each cell in each city, we used the estimated cooling impact, average energy use intensity, and building footprint to quantify the energy savings provided by trees (Equation (2)):

$$CoolingEnergySaving = CI*0.04*BF*KBTU \quad (2)$$

where *CI* is cell-level cooling impact, *BF* is cell-level building footprint, and *KBTU* is the average energy use intensity of the area. Third, we aggregated all cell-level cooling energy savings by land-cover and land-use types. In our supply and use tables for each city, we reported total supply of cooling energy savings stratified by land cover (ecosystem types, in physical and monetary supply tables) and cooling energy use (land use classified by NAICS categories, in physical and monetary use tables). Finally, we used average electricity cost for each state per kWh in 2019 U.S. dollars (U.S. Energy Information Administration, 2019) to monetize the value of electricity savings provided by urban trees for building cooling systems. We used the above-mentioned error propagation approach to generate confidence intervals for both physical and monetary supply of energy savings from cooling by trees.

2.3. Rainfall interception model

We based our rainfall interception model on the approach developed by Wang et al. (2008), which is also the basis for the i-Tree rainfall interception model (Hirabayashi, 2013). In this model, the key parameter is the LAI. The maximum capacity for rainfall interception by each square meter of tree cover is 0.0002 m times LAI. Also, the fraction of rainfall that would be intercepted (before reaching saturation) is calculated based on LAI. The i-Tree model uses high-resolution data and separates interception above impervious surfaces. We did not separate interception over impervious surfaces using unique grid-cell values because the NLCD tree cover and impervious cover datasets present only percent cover per 30 m grid cell without providing the exact overlap of these two. We used daily rainfall events data from Climate Data Online (National Centers for Environmental Information, 2018) for all available weather stations in the continental U.S. (hourly data are available from a smaller number of stations with more limited availability for 2011). If no storm data were found within an EAA, we expanded the search radius to 4.8 km, which allowed rainfall data to be compiled for all U.S. cities. First, we separated rainfall events by date(s) (Fig. 4). We used the MODIS seasonality layers to assign a leaf-on and leaf-off date to each station, which allowed us to assign leaf-on and leaf-off flags to each rainfall event.

We used three LAI values to calculate interception, providing a sensitivity analysis for the interception model. First, we used LAI raster data from Copernicus Global Land Service Catalog (Copernicus Global Land Service, 2020) for both leaf-on and leaf-off times. Since the resolution of this layer is low for urban areas (300 m), we observed a general underestimation of LAI, relative to higher resolution LAI data sources. The second LAI value we chose was a uniform value of 4.9, based on i-Tree Hydro's database (U.S. Department of Agriculture and Davey Tree, 2020) for urban areas. We adjusted this value for leaf-off time to 2.9 (Scurlock et al., 2001). Since the Copernicus LAI values are generally lower than their i-Tree counterparts, we took the Copernicus values as the lower bound of interception. To create an upper bound for our estimations, we used i-Tree average values plus 10% (5.39 and 3.19 for leaf-on and -off seasons, respectively). To generate cell-level results, we multiplied estimated interception in meters by the area of tree cover in the cell. In addition to interception, we also calculated total annual canopy rainfall (total annual precipitation at the canopy's top surface) as a reference point that allowed estimation of the percentage of intercepted water. We used municipal boundaries as EAAs for this service, but as a demonstration also summarized results at the HUC 10 scale for Denver, CO.

Hirabayashi (2013) describes methods for valuing rainfall interception using i-Tree, an approach we also follow. Hirabayashi estimates a U.S. national average value of $0.009 per gallon of avoided runoff, based on stormwater control costs for 16 U.S. cities across the nation's climate zones. In 2019 dollars, this value is $2.58 per m^3. To estimate rainfall interception over impervious surfaces (which is appropriate to value, as opposed to rainfall that would eventually be infiltrated by ground-level vegetation and soils), we followed Hirabayashi (2013) in assuming that impervious surfaces cover 25.5% of urban areas (Nowak & Greenfield, 2012). Since the SEEA EEA only allows valuation of ecosystem services that enter physical supply and use accounts (i.e., have a direct beneficiary), we only estimate the value of interception to wastewater treatment plants in cities with CSO systems. While this method is an adequate one used in recent i-Tree applications, a more accurate valuation of avoided runoff would use high-resolution tree cover and impervious surface data (which are unavailable nationally) to measure the fraction of interception service over impervious surfaces.

2.4. Accounting tables

We used cell-level results to aggregate values by ecosystem type (using land cover type data as a proxy), land use type (for use tables), and EAA. Using these aggregations, we built the following accounting tables:

a- Ecosystem extent table: Ecosystem service provision is a function of ecosystem extent and condition (United Nations, 2017). To aid in interpretation of ecosystem condition and supply and use tables, we created a table reporting ecosystem extent for each EAA.
b- Condition table: For 638 cities without CSO systems, we included the amount of rainfall interception in the condition table. This represents generalized benefits to water quality and regulation of the urban hydrograph that cannot be attributed to a particular end user (i.e.,

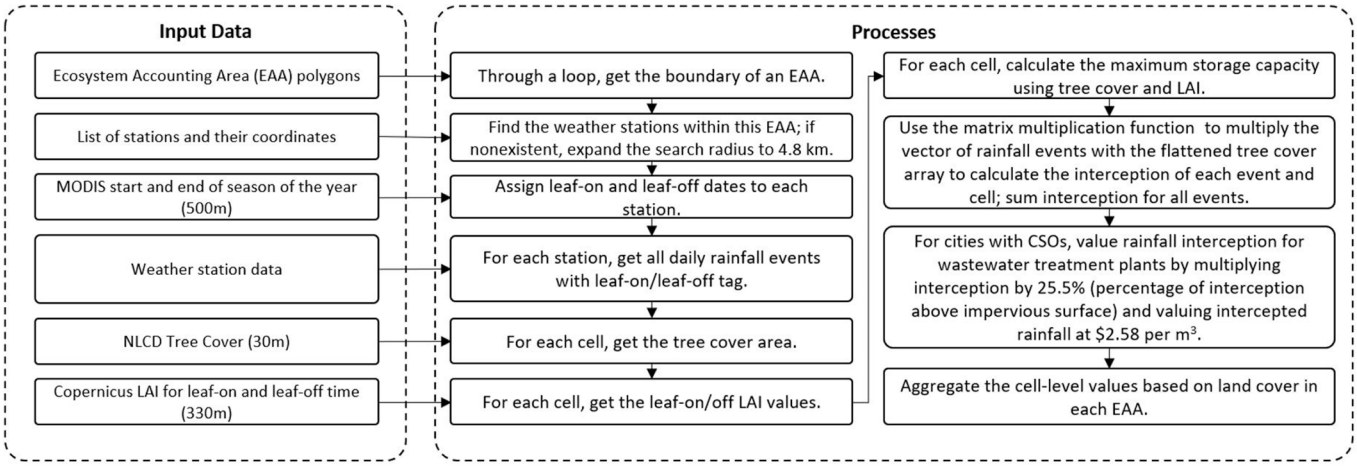

Fig. 4. Algorithm to estimate rainfall interception by trees. CSO: combined sewer overflow; LAI: leaf area index; MODIS: Moderate Resolution Imaging Spectroradiometer; NLCD: National Land Cover Database.

wastewater treatment), a functional state characteristic for ecosystem condition accounts (United Nations et al., 2020).

c- Physical supply table: This table reports the amount of energy savings (in GWh) and intercepted rainfall (m^3 of water) for each ecosystem type. Since the main beneficiary for rainfall interception are municipalities with CSO systems (130 cities), we included interception in the physical supply table only for those cities.

d- Physical use table: To quantify ecosystem service use by specific users (i.e., industries, households, government), we used the amount of energy savings (in GWh), aggregated by land use type to build the physical use table. Since the main final user of rainfall interception in CSO-system cities is wastewater treatment plants, we assigned all intercepted water to wastewater treatment in these cities.

e- Monetary supply table: We monetized the supply of energy savings and rainfall interception provided by different ecosystem types in 2019 U.S. dollars in the monetary supply table.

f- Monetary use table: For the monetary use table, we used land-use data to assign energy savings by economic unit, in dollars. We attribute all monetary values for rainfall interception to wastewater treatment plants only for cities with CSOs.

2.5. Sensitivity analysis

In addition to reporting uncertainty for both models, we evaluated how uncertainty in the NLCD tree canopy layer, a critical dataset in our analysis, affects model results for three cities in widely different climate zones. Since our temperature data are observed rather than estimated values, we did not assign any uncertainty to them. However, if the uncertainty ranges of each dataset were available to us, we could have incorporated them in the error propagation. We used high-resolution (1 m) vector tree canopy datasets for Denver, CO (Heris & Troy, 2018), New York, NY (New York City, 2017), and Seattle, WA (City of Seattle, 2016) to quantify differences with the NLCD-tree canopy-derived model outputs in these cities. These high-resolution tree canopy cover data are produced from lidar data and high-resolution leaf-on and leaf-off imagery. NLCD tree canopy data underestimate tree cover in all three cities (Coulston et al., 2012) and a comparison of the results for these cities can show the magnitude of change when higher-resolution data are available.

2.6. Code availability

We used Python to develop our models. Our models used open-source libraries such as Numpy, Rasterio, Fiona, Shapely, h5py, Scipy, Pandas, Scikit Learn, and Statmodels. We used Numpy arrays and Pandas dataframes extensively to speed up the algorithms. To manage national raster datasets, we used Hierarchical Data Format files for efficient Windows-based reading and writing. The code is available within a public code repository (U.S. Geological Survey, 2020).

3. Results

The results of both models are organized in multiple accounting tables. We report results for ecosystem extent (Table 1), condition (Table 2), physical supply and use (Tables 3 and 4), and monetary supply and use (Tables 5 and 6; Fig. 1). For the heat mitigation model, we only report results for cities with valid regression results (i.e., negative relationship between tree cover and heat; n = 736 out of 768). For the rainfall interception model, we report the results for cities with CSO systems (130 cities, in supply and use tables) and those without CSO systems (638 cities, in the condition table).

3.1. Heat mitigation

We quantified the aggregate cooling energy savings from trees in 736 U.S. cities to be approximately 4,098 and 4,229 GWh in 2011 and 2016, respectively (Table 3). The value of these electricity savings was $523 million in 2011 and $539 million in 2016 (Table 5). Cities with the highest energy savings in 2016 were Los Angeles, CA, Charlotte, NC, and Jacksonville, FL ($16.5, $15.5, and $15.1 million, respectively, Table 7). Eight of the top 10 cities for energy savings were in the top 30 by population (Table 7), including cities in the Southeast and Southwest (Fig. 5).

The supply table for energy savings from trees shows that the largest benefits were produced in the low-density developed land cover type (Table 3). In all 736 cities for 2016, 1,970 GWh of electricity savings were supplied by trees in low-density developed areas, with 1,229, 633, and 42 GWh supplied by trees in developed open space, medium-density developed, and high-density developed land cover areas, respectively. Energy savings in other land-cover types were much lower than in developed areas. The small numbers result from more scattered building presence in land cover types like forests and other open space. We observed similar patterns for physical supply of energy savings by ecosystem type for Colorado (17 cities with population of 50,000 or more) and Denver.

Table 5 shows the monetized values of energy savings provided by each ecosystem type. Since the final users of energy savings from trees are residents or other building owners or managers, land-use data inform our use table (Table 6). Over 95% of use in the monetary use table was associated with households. Other users such as offices, retail,

Table 1
Ecosystem extent table (km^2 per ecosystem accounting area and ecosystem type).

Ecosystem Accounting Area	Year	Ecosystem Types (Land cover)															
		Open Water	Developed - Open	Developed - Low	Developed - Medium	Developed - High	Barren	Deciduous Forest	Evergreen Forest	Mixed Forest	Scrub/Shrub	Grassland/Herbaceous	Pasture/Hay	Cultivated Crops	Woody Wetlands	Emergent Herbaceous Wetlands	Total
768 cities with population >=50k	2011	14,813	33,355	39,145	32,207	13,085	1,825	17,070	9,249	3,045	24,913	15,773	12,626	20,119	10,010	4,191	254,673
	2016	15,271	31,796	39,739	33,179	13,442	1,660	14,643	9,538	6,039	24,057	14,286	13,145	19,910	10,406	4,315	254,673
638 cities with population >=50k and without CSOs	2011	11,228	26,611	30,574	25,509	9,468	1,473	11,329	7,915	2,351	24,319	14,938	9,764	16,992	9,004	3,726	207,334
	2016	11,636	25,353	31,110	26,381	9,803	1,402	9,666	8,304	4,232	23,384	13,705	10,008	17,033	9,330	3,851	207,334
130 cities with CSOs with population >=50k	2011	3,585	6,744	8,571	6,698	3,617	352	5,741	1,334	694	593	836	2,862	3,127	1,007	465	47,339
	2016	3,635	6,443	8,629	6,798	3,639	258	4,977	1,234	1,807	673	581	3,137	2,877	1,076	464	47,339
736 cities with population >=50k and valid heat regression results	2011	14,641	32,638	38,194	31,426	12,853	1,778	17,066	9,220	3,039	19,983	15,347	12,576	19,022	9,859	4,064	244,510
	2016	15,067	31,122	38,796	32,376	13,202	1,308	14,639	9,508	6,034	19,587	13,701	13,118	18,788	10,260	4,200	244,510
Cities of Colorado (17 with population >=50k)	2011	127	759	1,290	829	282	22	26	239	1	426	1,838	129	1,181	157	64	7,369
	2016	141	814	1,310	864	296	8	13	207	2	445	1,961	73	1,046	59	131	7,369
Denver, CO	2011	24	173	340	223	108	4	3	1	0	4	190	16	303	25	3	1,417
	2016	25	172	342	228	110	1	1	0	0	15	197	5	296	8	16	1,417

Table 2
Ecosystem condition table: rainfall interception for the U.S., 17 cities in Colorado, and Denver (cities without combined sewer systems).

Ecosystem Accounting Area	Service Type	Year	Ecosystem Types (Land cover)															
			Open Water	Developed - Open	Developed - Low	Developed - Medium	Developed - High	Barren	Deciduous Forest	Evergreen Forest	Mixed Forest	Scrub/Shrub	Grassland/Herbaceous	Pasture/Hay	Cultivated Crops	Woody Wetlands	Emergent Herbaceous Wetlands	Total
638 cities with population >=50k and without CSOs	Rainfall Interception ($m^3 * 10^6$)	2011	3.0	369.3	200.4	37.6	2.6	1.1	265.4	274.4	108.3	35.3	32.3	21.3	7.3	387.4	17.8	1763.4
		2016	1.3	407.0	224.7	44.0	3.0	1.2	290.2	313.3	118.5	39.3	36.0	24.0	8.2	450.9	18.7	1982.0
Cities of Colorado (17 with population >=50k)		2011	0.0	2.1	4.6	1.2	0.0	0.0	0.3	1.7	0.0	1.3	0.2	0.0	0.0	0.2	0.1	11.9
		2016	0.0	2.1	4.6	1.2	0.0	0.0	0.2	1.6	0.0	1.0	0.2	0.0	0.0	0.2	0.1	11.4
Denver, CO		2011	0.0	0.4	0.8	0.2	0.0	0.0	0.0	0.0	0.0	0.0	0.0	0.0	0.0	0.0	0.0	1.4
		2016	0.0	0.4	0.7	0.2	0.0	0.0	0.0	0.0	0.0	0.0	0.0	0.0	0.0	0.0	0.0	1.3

Table 3
Physical supply table for the U.S., 17 cities in Colorado, and Denver. No cities in Colorado have Combined Sewer Overflow systems, so no rainfall interception results appear for these ecosystem accounting areas in the supply table.

Ecosystem Accounting Area	Service Type	Year	Ecosystem Types (Land cover)															
			Open Water	Developed - Open	Developed - Low	Developed - Medium	Developed - High	Barren	Deciduous Forest	Evergreen Forest	Mixed Forest	Scrub/Shrub	Grassland/Herbaceous	Pasture/Hay	Cultivated Crops	Woody Wetlands	Emergent Herbaceous Wetlands	Total
736 cities with population >=50k and valid regression results	Energy Savings (GWh)	2011	0.0	1,224.6	1,891.8	596.4	41.2	0.9	124.0	107.1	24.5	25.3	20.9	10.3	3.2	25.4	2.8	4,098.4
		2016	0.0	1,228.8	1,970.8	633.1	42.3	1.5	104.3	104.9	62.0	21.5	14.7	14.8	3.4	24.2	3.0	4,229.3
130 cities with CSOs with population >=50k	Rainfall Interception over Impervious Surfaces ($m^3 * 10^6$)	2011	0.3	33.2	23.1	6.5	0.5	0.1	60.3	11.3	18.4	1.1	0.9	3.4	0.3	8.0	0.6	168.0
		2016	0.2	32.4	22.9	6.7	0.5	0.1	57.9	11.7	18.1	0.7	0.8	3.2	0.3	8.4	0.6	164.6
Cities of Colorado (17 with population >=50k)	Energy Savings (GWh)	2011	0.0	24.5	104.1	32.1	1.0	0.0	0.7	1.1	0.0	1.9	0.3	0.0	0.0	0.9	0.1	166.6
		2016	0.0	24.4	105.8	32.5	1.0	0.0	0.5	1.4	0.1	2.2	0.4	0.0	0.0	0.5	0.2	169.1
Denver, CO	Energy Savings (GWh)	2011	0.0	8.0	27.1	6.6	0.3	0.0	0.0	0.0	0.0	0.0	0.0	0.0	0.0	0.1	0.0	42.2
		2016	0.0	7.9	26.9	6.6	0.3	0.0	0.0	0.0	0.0	0.0	0.0	0.0	0.0	0.0	0.0	41.9

and educational building owners received 1% or less of the total benefits. Without having accurate building type data (size and use), we recommend a cautious interpretation of the results. Since these use types are more likely to be located in multi-story buildings, their actual values could be larger.

3.2. *Rainfall interception*

Total modeled intercepted water for 768 cities was 2,422 and 2,627 million m^3 for 2011 and 2016, respectively. Most of the interception was in eastern cities, particularly in the Southeast (Fig. 6). However, only 25–27% of interception occurred in cities with CSO systems, which we

Table 4
Physical use table for the U.S., 17 cities in Colorado, and Denver. No cities in Colorado have Combined Sewer Overflow systems, so no rainfall interception results appear for these ecosystem accounting areas in the supply table.

Ecosystem Accounting Area	Service Type	Year	Economic Units												
			NAICS 11 Livestock	Wastewater treatment 221320	NAICS 31-33 Manufacturing	NAICS 44-45 Retail	NAICS 48-49 Transport warehousing	NAICS 51-56 Offices	NAICS 61 Educational services	NAICS 62 Health care & social assistance	NAICS 71 Entertainment	NAICS 92 Government	Households (No NAICS Code)	No NAICS equivalent	Total
736 cities with population >=50k and valid regression results	Energy Savings (GWh)	2011	0.3	0.0	9.6	16.5	89.2	21.6	24.2	7.4	1.4	6.9	3,906.3	15.1	4,098.4
		2016	0.2	0.0	9.3	15.8	87.8	21.3	24.7	7.4	1.4	7.2	4,039.1	15.0	4,229.3
130 cities with CSOs with population >=50k	Rainfall Interception over Impervious Surfaces ($m^3 * 10^6$)	2011	0.0	168.0	0.0	0.0	0.0	0.0	0.0	0.0	0.0	0.0	0.0	0.0	168.0
		2016	0.0	164.6	0.0	0.0	0.0	0.0	0.0	0.0	0.0	0.0	0.0	0.0	164.6
Cities of Colorado (17 with population >=50k)	Energy Savings (GWh)	2011	0.0	0.0	0.1	0.4	0.2	14.4	0.7	0.3	0.1	0.6	147.0	2.7	166.6
		2016	0.0	0.0	0.1	0.4	0.2	14.5	0.7	0.3	0.1	0.6	149.4	2.7	169.1
Denver, CO	Energy Savings (GWh)	2011	0.0	0.0	0.0	0.1	0.1	4.6	0.3	0.1	0.1	0.6	35.7	0.6	42.2
		2016	0.0	0.0	0.0	0.1	0.1	4.6	0.3	0.1	0.1	0.6	35.4	0.6	41.9

Table 5
Monetary supply table for the U.S., 17 cities in Colorado, and Denver.

Ecosystem Accounting Area	Service Type	Year	Ecosystem Types (Land cover)															
			Open Water	Developed - Open	Developed - Low	Developed - Medium	Developed - High	Barren	Deciduous Forest	Evergreen Forest	Mixed Forest	Scrub/Shrub	Grassland/Herbaceous	Pasture/Hay	Cultivated Crops	Woody Wetlands	Emergent Herbaceous Wetlands	Total
736 cities with population >=50k and valid regression	Energy Savings (Million $)	2011	0.0	150.2	238.4	87.0	6.3	0.1	14.8	12.4	3.0	3.2	2.4	1.2	0.4	3.1	0.3	522.7
		2016	0.0	150.5	247.7	91.8	6.5	0.2	12.4	12.2	7.5	2.8	1.7	1.7	0.5	2.9	0.4	538.6
Cities of Colorado (17 with population >=50k)		2011	0.0	2.9	12.5	3.9	0.1	0.0	0.1	0.1	0.0	0.2	0.0	0.0	0.0	0.1	0.0	20.0
		2016	0.0	2.9	12.7	3.9	0.1	0.0	0.1	0.2	0.0	0.3	0.0	0.0	0.0	0.1	0.0	20.3
Denver, CO		2011	0.0	1.0	3.3	0.8	0.0	0.0	0.0	0.0	0.0	0.0	0.0	0.0	0.0	0.0	0.0	5.1
		2016	0.0	0.9	3.2	0.8	0.0	0.0	0.0	0.0	0.0	0.0	0.0	0.0	0.0	0.0	0.0	5.0
130 cities with CSOs with population >=50k	Avoided Runoff Value (Million $)	2011	0.7	85.6	59.7	16.9	1.2	0.4	155.7	29.1	47.4	2.8	2.2	8.7	0.9	20.7	1.6	433.6
		2016	0.6	83.7	59.0	17.4	1.2	0.4	149.4	30.2	46.6	1.9	2.1	8.2	0.9	21.6	1.6	424.7

Table 6
Monetary use table for the U.S., 17 cities in Colorado, and Denver.

Ecosystem Accounting Area	Service Type	Year	Economic units												
			NAICS 11 Livestock	Wastewater treatment 221320	NAICS 31-33 Manufacturing	NAICS 44-45 Retail	NAICS 48-49 Transport warehousing	NAICS 51-56 Offices	NAICS 61 Educational services	NAICS 62 Health care & social assistance	NAICS 71 Entertainment	NAICS 92 Government	Households (No NAICS Code)	No NAICS equivalent	Total
736 cities with population >=50k and valid regression results	Energy Savings (Million $)	2011	0.0	0.0	1.3	2.1	11.3	2.9	3.5	0.9	0.2	0.9	497.7	1.8	522.7
		2016	0.0	0.0	1.3	2.1	11.2	2.9	3.5	1.0	0.2	0.9	513.7	1.8	538.6
Cities of Colorado (17 with population >=50k)		2011	0.0	0.0	0.0	0.1	0.0	1.7	0.1	0.0	0.0	0.1	17.6	0.3	20.0
		2016	0.0	0.0	0.0	0.1	0.0	1.7	0.1	0.0	0.0	0.1	17.9	0.3	20.3
Denver, CO		2011	0.0	0.0	0.0	0.0	0.0	0.6	0.0	0.0	0.0	0.1	4.3	0.1	5.1
		2016	0.0	0.0	0.0	0.0	0.0	0.5	0.0	0.0	0.0	0.1	4.3	0.1	5.0
130 cities with CSOs with population >=50k	Avoided Runoff Value (Million $)	2011	0.0	433.6	0.0	0.0	0.0	0.0	0.0	0.0	0.0	0.0	0.0	0.0	433.6
		2016	0.0	421.6	0.0	0.0	0.0	0.0	0.0	0.0	0.0	0.0	0.0	0.0	424.7

valued at $433.6 and $424.7 million for 2011 and 2016, respectively (Tables 2–5). Modeled rainfall interception for four cities in Arizona (Avondale, Buckeye, Goodyear, Yuma) was zero due to gaps in the NLCD tree canopy cover dataset in those parts of the state for both years. Since rainfall interception is calculated based on localized, individual storm events for each city, interpreting change between years with very different weather patterns can be challenging. In some cities where the rainfall patterns in 2011 and 2016 were similar (length and frequency of storms), the amount of interception is also similar. For example, about 6% of rainfall was intercepted in Chicago in both 2011 and 2016 (about 4 million m^3). By contrast, due to differing weather patterns between years, intercepted rainfall in 2016 for San Antonio, TX, was almost twice

Table 7
Summary of heat mitigation and rainfall interception results for the 30 largest cities in the U.S. * indicates cities with Combined Sewer Overflow systems. CI: confidence interval; LAI: leaf area index.

City	Population	Average Cooling Energy Use (KBTU)	Electricity Cost ($/ KWh)	Energy Savings (million $)						Rainfall Interception ($m^3 * 10^6$)							
				2011			2016			2011				2016			
				Lower CI (95%)	Mean	Upper CI (95%)	Lower CI (95%)	Mean	Upper CI (95%)	Copernicus LAI	i-Tree LAI Average	i-Tree +10%	Total Canopy Rain	Copernicus LAI	i-Tree LAI Average	i-Tree +10%	Total Canopy Rain
New York, NY*	8,175,133	17	0.18	1.1	1.1	1.2	1.3	1.4	1.5	5.0	11.0	12.0	268.5	5.2	11.4	12.4	179.0
Los Angeles, CA	3,792,621	14	0.20	14.4	16.5	18.6	14.5	16.6	18.7	1.4	4.8	5.2	79.4	1.0	3.5	3.8	65.4
Chicago, IL*	2,695,598	15	0.13	2.3	2.4	2.5	2.3	2.4	2.5	1.3	4.3	4.6	68.2	1.2	3.9	4.3	63.3
Houston, TX	2,099,451	21	0.12	1.7	2.0	2.4	1.5	1.9	2.2	13.2	30.8	33.6	754.1	18.6	42.1	46.1	1,673.7
Philadelphia, PA*	1,526,006	27	0.14	1.0	1.0	1.1	1.0	1.1	1.1	3.5	6.3	6.9	150.5	3.0	5.8	6.3	94.7
Phoenix, AZ	1,445,632	30	0.12	0.0	0.0	0.0	0.0	0.0	0.0	0.0	0.0	0.0	0.0	0.0	0.0	0.0	0.0
San Antonio, TX	1,327,407	21	0.12	5.3	5.9	6.6	5.4	6.0	6.7	7.2	20.5	22.3	415.5	13.4	39.1	42.7	1,258.7
San Diego, CA	1,307,402	14	0.20	4.4	5.1	5.7	4.5	5.2	5.9	0.6	2.3	2.5	27.9	0.5	2.1	2.2	26.3
Dallas, TX	1,197,816	21	0.12	3.9	4.2	4.6	3.9	4.3	4.7	5.3	19.1	20.8	468.8	9.0	30.5	33.4	825.9
San Jose, CA	945,942	14	0.20	1.8	2.0	2.3	1.8	2.1	2.3	0.6	1.9	2.0	22.0	0.5	1.6	1.7	27.8
Jacksonville, FL	821,784	22	0.12	12.3	14.0	15.8	13.1	15.1	17.1	127.4	199.9	218.4	5,429.6	132.3	204.7	223.8	5,668.9
Indianapolis, IN*	820,445	23	0.12	5.7	6.2	6.6	5.8	6.2	6.7	13.8	25.8	28.1	468.3	12.0	21.3	23.2	431.6
San Francisco, CA*	805,235	14	0.20	0.1	0.1	0.1	0.1	0.1	0.1	0.2	0.4	0.4	5.3	0.2	0.4	0.4	8.1
Austin, TX	790,390	21	0.12	9.1	10.5	11.9	9.2	10.6	12.0	10.1	29.0	31.4	425.6	18.3	54.8	59.7	1,549.9
Columbus, OH*	787,033	20	0.12	2.1	2.3	2.5	2.1	2.3	2.4	6.3	13.2	14.4	233.0	5.2	10.7	11.7	152.3
Fort Worth, TX	741,206	21	0.12	2.0	2.3	2.5	2.1	2.3	2.5	2.6	9.8	10.7	217.7	3.3	12.5	13.6	309.8
Charlotte, NC	731,424	31	0.12	12.9	14.6	16.3	13.6	15.5	17.4	21.2	50.1	54.8	1,060.8	20.5	47.0	51.3	965.1
Detroit, MI*	713,777	14	0.15	0.8	0.8	0.9	0.8	0.8	0.9	1.7	4.6	5.0	71.9	1.6	4.2	4.5	51.1
Memphis, TN	646,889	33	0.11	4.9	5.3	5.7	5.0	5.4	5.9	19.7	39.4	43.1	1,025.8	20.2	38.9	42.6	980.8
Baltimore, MD*	620,961	20	0.13	1.1	1.3	1.4	1.2	1.3	1.4	2.4	4.8	5.3	101.8	1.8	3.9	4.2	59.6
Boston, MA*	617,594	16	0.23	1.5	1.6	1.8	1.6	1.8	2.0	1.4	3.1	3.4	51.4	1.2	2.9	3.2	35.8
Seattle, WA*	608,660	30	0.09	1.8	2.0	2.3	2.3	2.7	3.1	2.4	6.9	7.5	64.0	2.2	6.5	7.1	78.5
Washington, DC*	601,723	9	0.13	0.5	0.5	0.6	0.5	0.5	0.6	1.8	3.8	4.1	59.8	1.7	3.6	3.9	47.2
Nashville, TN*	601,222	33	0.11	6.4	7.3	8.1	6.4	7.4	8.3	79.8	118.8	129.5	2,832.2	80.3	114.0	124.5	2,632.5
Denver, CO	600,158	16	0.12	3.5	5.1	6.6	3.5	5.0	6.5	0.4	1.4	1.6	14.6	0.4	1.3	1.4	13.4
Louisville, KY*	597,337	28	0.10	2.7	3.0	3.2	2.8	3.0	3.3	31.1	47.9	52.4	1,148.3	29.6	44.5	48.6	864.4
Milwaukee, WI*	594,833	14	0.14	1.4	1.5	1.6	1.5	1.6	1.6	1.4	4.4	4.8	55.8	1.7	5.1	5.6	64.8
Portland, OR*	583,776	19	0.11	4.0	5.3	6.6	4.1	5.4	6.8	8.9	16.8	18.3	182.3	8.8	17.1	18.7	262.0
Las Vegas, NV	583,756	25	0.12	0.5	0.7	0.9	0.5	0.7	0.9	0.0	0.0	0.0	0.1	0.0	0.0	0.0	0.1
Oklahoma City, OK	579,999	34	0.10	4.7	5.2	5.8	4.8	5.3	5.8	15.3	36.2	39.4	820.3	19.4	45.0	49.1	899.9
Albuquerque, NM	545,852	17	0.13	4.0	8.2	12.5	4.0	8.2	12.5	0.1	0.8	0.8	6.4	0.2	1.1	1.1	8.9

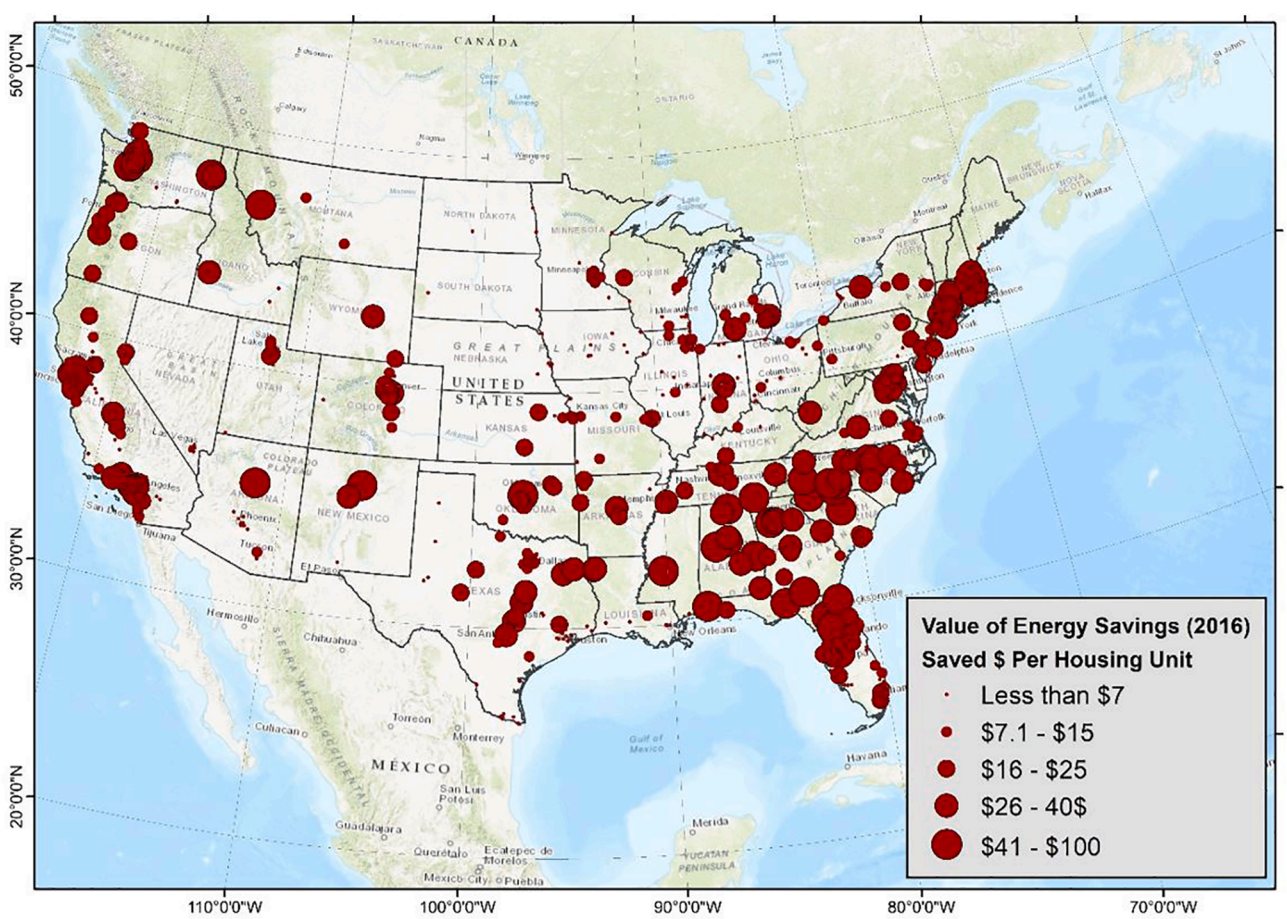

Fig. 5. Value of energy savings ($ per housing unit) in 2016 for U.S. cities with population over 50,000.

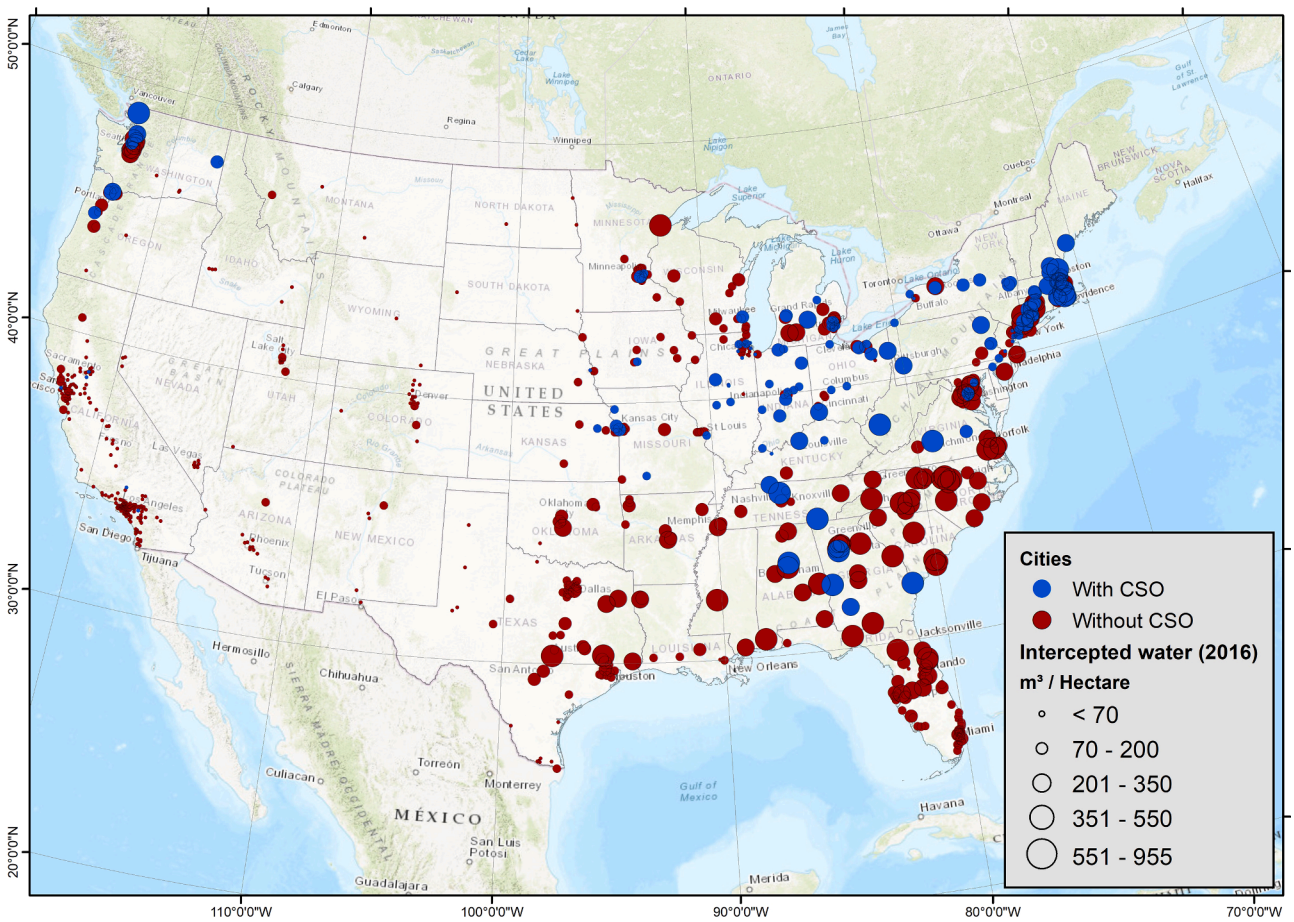

Fig. 6. Intercepted rainfall (m^3 per Ha) in 2016 for U.S. cities with population over 50,000.

that of 2011 (20 vs 39 million m^3), though the percentage of rainfall intercepted declined (from 4.9 to 3.1%). In 2016, the three cities with the highest amount of intercepted rainfall were Jacksonville, FL (204 million m^3), Nashville, TN (113 million m^3), and Suffolk, VA (94 million m^3).

Our condition and supply tables for rainfall interception show that, as expected, forests, developed open spaces, and woody wetlands provided the most total interception in all cities (Tables 2 and 3). Also as expected, a negative relationship exists between total interception and development density. More interception occurred in low-density (developed-low and developed-open) areas (852.5 million m^3 nationally in 2016), though high-density developed areas still provided 4.9 million m^3 nationally in 2016, which is important considering that increased runoff in these areas could increase wash-off of hazardous pollutants. Comparing nationwide values with those for Colorado showed differences between national and state-specific urban landscape characteristics. Unlike the national total, the greatest interception for Colorado cities did not occur in forest ecosystem types, but in low-density developed areas. This reflects the fact that trees in Colorado are mostly planted and maintained in urban areas; Colorado cities generally lack natural forested areas as do cities in the East or Pacific Northwest. Results for Denver showed the same pattern, with over 50% of interception occurring in low-density developed areas. This shows how comparing results for cities (EAAs) of different sizes, urban morphologies, and climates provides insight for understanding urban ecosystem service patterns.

Since the final beneficiaries of rainfall interception in cities with CSOs are sewage treatment facilities (NAICS code 221320), we assigned all use of this ecosystem service to that industry, calculated in physical and monetary terms based on interception over impervious surfaces (Tables 4 and 5).

3.3. Watershed-scale rainfall interception analysis

To illustrate how the use of different EAAs can aid the interpretation of rainfall interception's role in the local water cycle, we summarized model results for Denver, CO, using HUC 10 watershed boundaries as EAAs. In this example, the intercepted rainfall outside of the city boundary still benefits water quality in the city through avoided runoff in upstream regions (Fig. 7). The majority of interception occurred outside the city boundary for all three watershed units, particularly in forest-covered areas. For instance, the greatest interception occurred in the Little Dry Creek watershed, with over 2.5 million m^3 of interception in 2016, 12% of which occurred within the city boundary (Table 8). The Little Dry Creek watershed has about 20 km^2 of tree cover outside the city limit and 3 km^2 of tree coverage within the city. Watershed units can thus reveal how cities benefit from ecosystem services that are generated outside the city limits.

3.4. Sensitivity analysis

To assess the accuracy of our results, we developed two types of sensitivity analyses. First, for each model, we provided lower and upper bound estimates. In the heat mitigation model, we used the propagated error of the regression models to produce confidence intervals at the alpha = 0.05 level (reported by ecosystem type in Table 9). In 2016, the mid-level value for energy savings for 736 cities was 4,229 GWh, with lower and upper bounds of 3,622 and 4,825 GWh, respectively. The main source of uncertainty in the rainfall interception model is related to LAI. The three LAI values that we used—based on remote-sensing data

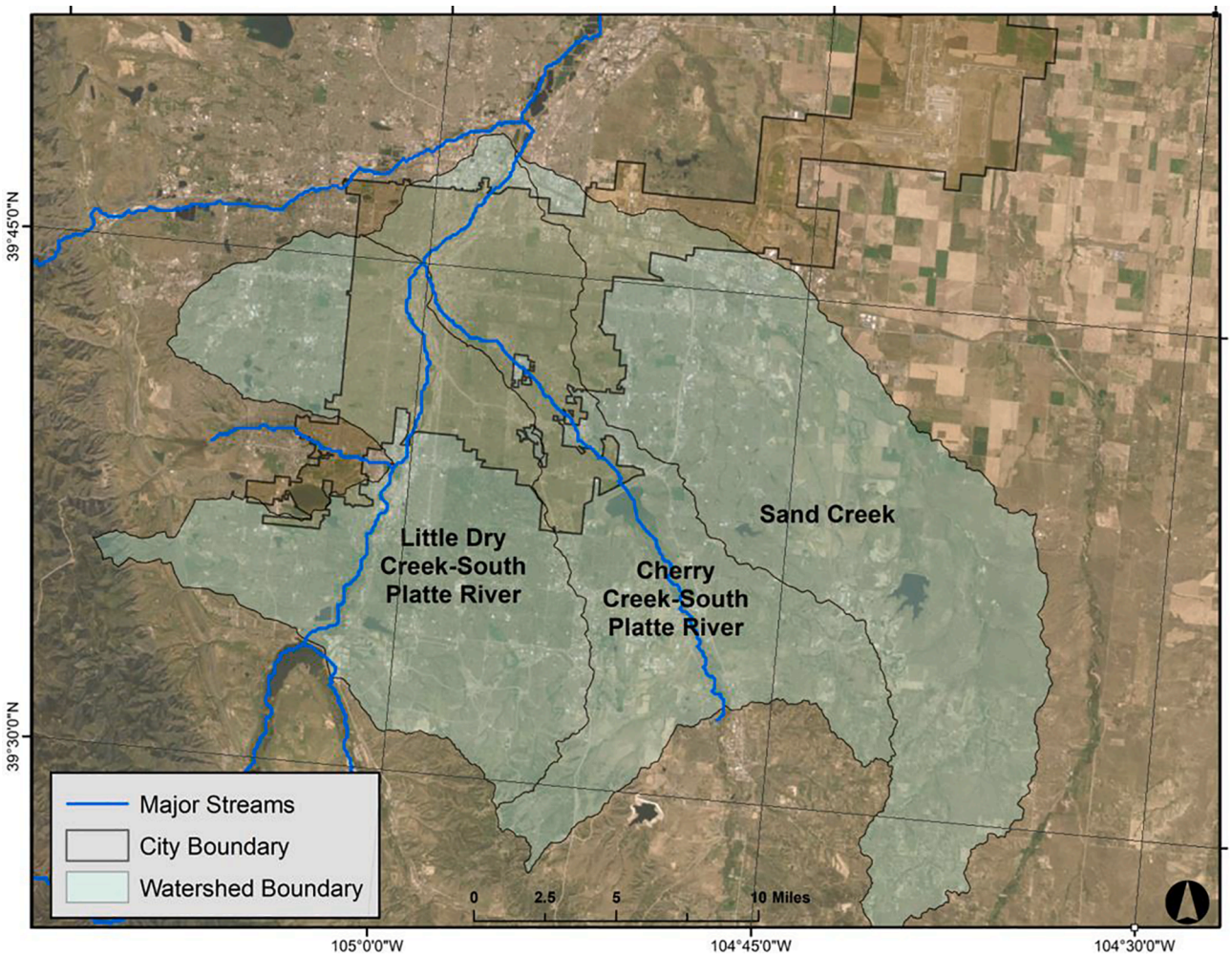

Fig. 7. Denver's HUC 10 watersheds.

Table 8
Rainfall interception in Denver HUC10 watersheds.

Ecosystem Accounting Area	Rainfall Interception (m^3 *10^6)			Total Tree Cover (km^2)		
	Within City Boundary	Outside City Boundary	% within city	Within City Boundary	Outside City Boundary	% within city
Cherry Creek-South Platte River	0.59	0.91	39.2%	5.1	7.2	41.5%
Little Dry Creek-South Platte River	0.30	2.22	12.1%	3.1	20.3	13.2%
Sand Creek	0.04	0.81	4.4%	0.5	6.7	6.9%

(Copernicus LAI), the i-Tree average, and i-Tree average + 10%—produced a relatively wide range of results, particularly for the lower bound. In 2016, interception for all cities based on mid-level LAI (i-Tree estimate) was 2,627 million m^3, while the lower bound (Copernicus LAI) was 1,425 m^3, and the upper bound (i-Tree average + 10%) is 2,868 m^3 (Table 9).

Moderate-resolution (30 m) tree canopy data are known to underestimate tree canopy cover in cities (Greenfield et al., 2009). When we replaced the NLCD tree canopy layer with a high-resolution (1 m) layer for New York, NY, Denver, CO, and Seattle, WA, energy savings and rainfall interception were substantially greater (Table 10). The results for energy savings more than doubled in Denver and New York City, and were 74% greater in Seattle. The rainfall interception model was similarly sensitive to the resolution of tree cover data.

4. Discussion

Our study shows how ecosystem accounts can quantify urban ecosystem services, their variation across different U.S. cities and regions, and how these benefits accrue to different users such as households, industries, and government. The results illustrate how people in the built environment interact with and benefit from different urban ecosystems. We also show how an ecosystem accounting framework can be applied to cities and summarized at the watershed, city, state, and national levels. Our results characterize urban ecosystem extent, condition, and services, contributing to a larger set of pilot SEEA accounts for the United States. These include national-scale accounts for land (Wentland et al., 2020), water (Bagstad et al., 2020), and a subnational ecosystem account for a 10-state region in the U.S. Southeast (Warnell et al., 2020). In an example for Atlanta, GA, Warnell et al. also illustrate how the results of accounts can be integrated to show population,

Table 9
Confidence intervals for energy savings and rainfall interception models. CI: Confidence interval, LAI: leaf area index.

Ecosystem Accounting Area	Service Type	Year	Sensitivity Analysis	Ecosystem types (Land cover)															
				Open Water	Developed - Open	Developed - Low	Developed - Medium	Developed - High	Barren	Deciduous Forest	Evergreen Forest	Mixed Forest	Scrub/Shrub	Grassland/Herbaceous	Pasture/Hay	Cultivated Crops	Woody Wetlands	Emergent Herbaceous Wetlands	Total
736 cities with population >=50k and valid regression results	Energy Savings (GWh)	2011	Lower CI (95%)	-	1,041.3	1,629.0	531.1	38.3	0.7	104.3	81.2	19.6	20.3	18.3	9.1	2.8	21.5	2.5	3,520.0
			Mean	-	1,224.6	1,891.8	596.4	41.2	0.9	124.0	107.1	24.5	25.3	20.9	10.3	3.2	25.4	2.8	4,098.4
			Upper CI (95%)	-	1,407.8	2,154.6	661.7	44.2	1.0	143.7	132.9	29.5	30.3	23.6	11.4	3.6	29.2	3.2	4,676.7
		2016	Lower CI (95%)	-	1,041.0	1,693.7	561.8	39.2	1.3	86.9	78.9	51.2	16.7	13.0	13.3	3.0	20.5	2.6	3,622.9
			Mean	-	1,228.8	1,970.8	633.1	42.3	1.5	104.3	104.9	62.0	21.5	14.7	14.8	3.4	24.2	3.0	4,229.3
			Upper CI (95%)	-	1,416.7	2,248.0	704.3	45.5	1.7	121.7	130.8	72.8	26.3	16.4	16.4	3.9	27.9	3.3	4,835.7
All 768 cities with population >=50k	Rainfall Interception (m^3 * 10^6)	2011	Copernicus LAI	1.9	219.4	106.4	19.8	1.2	0.6	316.1	188.7	109.4	19.0	15.6	18.1	4.8	278.3	9.4	1,308.7
			i-Tree LAI Average	4.1	499.4	291.1	63.3	4.4	1.7	502.0	318.5	180.4	39.5	35.7	34.6	8.6	418.9	20.2	2,422.2
			i-Tree +10%	4.4	544.9	317.4	68.9	4.8	1.9	547.5	347.6	196.8	43.1	38.9	37.7	9.4	457.1	22.0	2,642.4
			Total Rainfall	79.2	9,798.8	5,230.0	1,027.3	71.6	32.8	10,104.7	6,659.4	3,496.0	762.0	749.3	706.4	159.1	8,963.7	435.3	48,275.5
		2016	Copernicus LAI	1.7	234.0	114.4	22.0	1.3	0.7	328.9	214.3	116.3	17.7	16.4	19.3	5.5	322.5	9.7	1,424.6
			i-Tree LAI Average	3.8	534.1	314.3	70.4	4.8	1.8	517.2	359.2	189.3	42.2	39.2	36.6	9.5	483.8	21.1	2,627.4
			i-Tree +10%	4.1	582.9	342.9	76.7	5.3	1.9	564.3	392.3	206.7	46.0	42.8	39.9	10.4	528.3	23.1	2,867.7
			Total Rainfall	81.7	10,972.5	6,008.3	1,188.7	80.3	36.4	9,734.7	8,750.1	3,777.8	953.3	844.0	765.8	213.3	12,082.8	513.3	56,003.1

Table 10
Sensitivity analysis using high-resolution vs. National Land Cover Database tree canopy cover data in ecosystem accounting models.

Ecosystem Accounting Area	Service Type	Input Tree Cover Data		Percent difference
		National Land Cover Database Tree Cover	High-Resolution Tree Cover	
Denver, CO	Energy Savings (GWh)	41.9	104.3	149.2%
	Rainfall Interception (m^3 *10^6)	0.4	1.3	259.0%
New York, NY	Energy Savings (GWh)	6.5	18.5	183.5%
	Rainfall Interception (m^3 *10^6)	5.0	8.2	62.5%
Seattle, WA	Energy Savings (GWh)	28.3	49.3	73.9%
	Rainfall Interception (m^3 *10^6)	2.2	4.7	108.5%

economic, and environmental trends for an urban area.

Periodic ecosystem accounts can inform policymaking processes at local, regional, and national levels. Since the outputs of our models are spatially explicit, they show the areas and users who benefit from tree cover the most or the least. With adequate time-series data, local planning institutions can monitor tree cover changes and their related ecosystem services to track the benefits that trees provide to communities. Recent declines in tree canopy cover, for instance, suggest losses of potentially important ecosystem services in cities (Nowak & Greenfield, 2018). Cities can identify vulnerable populations that could benefit the most from trees in extreme weather events (Declet-Barreto et al., 2016). Cities can also use such data to guide and prioritize their green infrastructure investments. For example, the city of Denver has mapped their tree cover (Heris & Troy, 2018) to evaluate the impact of the city's tree canopy cover loss from emerald ash borer. In another example, Sacramento, CA, has mapped their tree cover and quantified rainfall interception (Center for Urban Forest Research, 2002) to inform their various tree-planting and maintenance programs (City of Sacramento CA, 2019). At a national scale, periodic ecosystem accounts can depict how climate-related trends interact with long-term planning efforts in cities across the country. Urban ecosystem accounts would help urban, regional, and Federal government entities monitor the role of investments, tree diseases, weather patterns, and ecosystem service changes in communities.

A primary contribution of this paper is in applying the ecosystem accounting approach to urban ecosystems at the national scale for a large, heterogeneous country with 768 medium- and large-sized cities, building from a relatively limited global experience base with urban ecosystem accounting. Modeling ecosystem services in urban areas is complex and challenging because of the heterogeneous nature and the variety of sizes, urban morphologies, climates, and socioeconomic characteristics of various beneficiaries in different cities (Keeler et al., 2019). To run our models, we developed and used high-resolution datasets, including large climate datasets. Spatial computation of such layers was intensive and required advanced spatial data analytics and programing. Although our study was only focused on two services, the platform that we created can be expanded to include additional ecosystem services such as carbon sequestration, air filtration, and noise mitigation provided by urban vegetation, similar to the work that has been carried out for the U.K. (Anderson, 2018).

In this study, we developed models explicitly designed to support the compilation of ecosystem accounts using the SEEA EEA framework. Numerous models for ecosystem services have been developed, including the impact of trees on rainfall and heat mitigation in urban areas (Keeler et al., 2019; Nowak et al., 2017; Zhou et al., 2017), and for other urban ecosystem services (Nowak & Dwyer, 2007). Our models enable (1) full customization of model inputs and parameters, which can be unique to each city (accounting for differences in e.g., cities' size or climate zone); (2) alignment of data on a consistent 30-m grid to minimize error and use consistent basic spatial units; (3) the automatic summation as direct model outputs of ecosystem service supply by ecosystem type, use by economic units, and aggregation by EAAs, even for a large number of EAAs (768 in our study); and (4) programming using Numpy arrays, which are fast and facilitate the recalculation of updated ecosystem accounts as new data become available. Ideally, these models should be updated annually, though current limitations may make updates every few years more realistic, as new data become available. These features make our models better suited to ecosystem accounting than most urban ecosystem service models.

A well-known challenge in developing models for urban ecosystem services is the complexity and heterogeneity of urban contexts. This heterogeneity has made previous researchers pessimistic about the

capacity of generalized toolkits to estimate the value of urban nature, due to the wide variety of factors that influence it (Keeler et al., 2019). One approach that we used in this paper was to localize models for each city. Both of our models are based on local data such as temperature, precipitation, and energy use. More sophisticated methods to modify these models on the fly could improve the results. We evaluated decision tree, random forest, and extra random forest models but realized that in order to create a robust model, each region would require specific parameters to produce meaningful results. Manual parameter adjustment for 768 cities would be impractical due to challenges in interpreting model coefficients, an inherent problem in machine-learning algorithms. However, machine learning is increasingly being applied to ecosystem services (Willcock et al., 2018) and offers one path forward in addressing the problem of context specificity in these relationships at both inter- and intra-city scales. A procedure to account for more model parameters would be a possible future improvement of our models.

A set of simplifying assumptions was necessary to apply urban ecosystem service models at the national scale. We tended to make conservative assumptions where appropriate data were not available. Both of our models used NLCD tree canopy data (2011 and 2016). Differences between NLCD tree canopy 2011 and 2016 were relatively small. However, the NLCD tree canopy dataset has an inherent underestimation (Greenfield et al., 2009), particularly in urban areas where built environments are heterogeneous and tree detection is more difficult. Our cooling energy savings results used different models with more conservative assumptions than comparable studies, yielding smaller values ($528 million vs. $1.0–1.6 billion by McDonald et al. (2020) and $4.7 billion by (Nowak et al., 2017)). Notably, we did not account for the role of trees in reducing mean radiant temperature through shading. Additionally, Nowak et al. adjusted NLCD tree canopy values using a sampling approach based on plot-scale data for 20 cities and encompassed a much larger area of "urban/community" land than our 768 cities. Finally, our sensitivity analysis suggests that the value of these services may be much higher if, for example, 1-m data were available for all 768 cities nationwide.

Future work could improve the simplifying assumptions and ecosystem accounting estimates of our models. Future versions of both models could take a wider view of ecosystem contributions to these services, by incorporating rainfall interception by shrubs and the effects of parks and other open space in providing heat mitigation. For the rainfall interception model, high-resolution data about tree species (coniferous vs. deciduous) and structure, canopy height, and impervious surface cover under the canopy could improve model accuracy, as could incorporation of hourly rainfall data. In addition, calculating the evaporation portion of interception using local climate data such as vapor pressure deficit, temperature, and wind intensity could improve the results.

For the heat mitigation model, incorporating wind and tree shade data could similarly improve results. Furthermore, the building component of the heat mitigation model has space for improvement through adding building use type and height information. We used building footprint area as a proxy for floor area to apply average cooling energy use values. However, our model underestimates energy savings in high-density areas where multi-story (2–4 floor) buildings have substantially higher floor area than footprint area; we expect that the energy savings impact of trees drops for high-rise buildings, however, as shaded building surface area declines. Applying residential average uses to all buildings also underestimates energy use in commercial and office buildings in moderate- to high-density areas. The impact of trees on building energy use could also be represented using a more complex relationship. For example, we assumed that buildings benefit only from being in the same grid cell with trees. In reality, the heat-mitigation impact of trees may extend beyond a 30-m grid cell. Our assumption is very conservative, so further experimental studies on the extent of trees' impact based on wind direction at a national scale or for various climate regions would be a helpful addition to this approach. Finally, further investigation of the relationship between temperature and tree canopy cover would be valuable in the 32 cities where we found a positive relationship between these variables.

Ecosystem service models used in accounting would ideally account for accurate, year-to-year changes over time in all model parameters. Land-use and building data, which are currently available only for a single year, are most limiting in this respect. Our building footprints dataset is based on data published by Microsoft in 2018, but without information about its base year. If such a dataset were updated in the future, knowing the base year would improve accounting results. Similarly, we used land-use data that are currently available only for the year 2010. Our models account for interannual weather differences. Similarly, in ecosystem accounts for the Southeast U.S., Warnell et al. (2020) use the method of Nowak et al. (2014) for quantifying air filtration change from 2010 to 2015. They use weather data for those years, but hold tree canopy constant, based on 2011 data. Future analysis could more fully isolate the relative influence of weather and tree canopy change in cooling and infiltration, running models using for instance the same NLCD tree cover data (2011 or 2016), with 3-year average weather data to quantify the relative influence of interannual climate variation on these urban ecosystem accounts.

Like most ecosystem accounts, this study relied heavily on remote sensing methods using Earth observation data (Tavares et al., 2019). Our data included well-established and frequently used products from MODIS and NLCD. Although NLCD's 30 m resolution introduces error in both data (Greenfield et al., 2009; Wickham et al., 2020) and ecosystem service model results (Section 3.4) in heterogeneous urban environments, its long-term record and national-scale availability remain valuable for urban ecosystem accounts. Adjustments to the tree canopy data may be able to remove bias and reduce error by about 5–10%, which can substantially improve the accuracy of ecosystem accounting assessments, though not to the accuracy levels provided by high-resolution (1 m) data. In addition, we developed novel data products from unprocessed Earth observation data, such as the national summer daytime surface temperature, which were not previously available at high resolution. We also demonstrated the value of the National Land Use Dataset (Theobald, 2014) for ecosystem accounting by aligning a national, 30 m land-use dataset with NAICS industrial classes in physical and monetary use tables. Finally, we adapted the Microsoft buildings dataset to better serve ecosystem accounting needs by developing a set of national building footprint data rasterized to a common grid with NLCD (Heris et al., 2020b). By integrating Earth observation products ranging from well established to entirely novel, we further illustrate the importance of Earth observation for ecosystem accounting (EO4EA, 2019).

5. Conclusion

In this study, we developed models for heat mitigation and rainfall interception to support urban ecosystem accounting in the U.S. We applied those models to quantify ecosystem services generated by trees in 768 U.S. cities with populations greater than 50,000. In addition to providing the first of several planned nationwide U.S. ecosystem accounts (Boyd et al., 2018), we advance urban ecosystem accounting by developing models specifically designed to produce SEEA EEA ecosystem extent, condition, and physical and monetary supply and use tables with automated aggregation by ecosystem types and EAAs. We used open-source, computationally fast libraries in our models and made them publicly available for reuse and adaptation in ecosystem accounting and ecosystem service modeling (U.S. Geological Survey, 2020). Given the time required to develop new ecosystem accounts and update them as new data become available, such shared data and model repositories offer an important path forward for increasing the use of ecosystem accounting in faster, more transparent ways.

Declaration of Competing Interest

The authors declare that they have no known competing financial interests or personal relationships that could have appeared to influence the work reported in this paper.

Acknowledgements

We acknowledge the support of the NASA Biodiversity and Ecological Forecasting Program (grant no. 80NSSC18K0341) for Heris' time. Support for Bagstad's time was provided by the U.S. Geological Survey's Land Change Science Program. This work was conducted as a part of the "Accounting for U.S. Ecosystem Services at National and Subnational Scales" working group supported by the National Socio-Environmental Synthesis Center under funding received from the National Science Foundation (grant no. DBI-1052875) and the U.S. Geological Survey John Wesley Powell Center for Analysis and Synthesis (grant no. GX16EW00ECSV00). The use of any trade, firm, or product names is for descriptive purposes only and does not imply endorsement by the U.S. Government.

Appendix A. Supplementary data

Supplementary data to this article can be found online at https://doi.org/10.1016/j.ecoser.2020.101226.

References

Akbari, H., Pomerantz, M., Taha, H., 2001. Cool surfaces and shade trees to reduce energy use and improve air quality in urban areas. Sol. Energy 70 (3), 295–310. https://doi.org/10.1016/S0038-092X(00)00089-X.

Aminipouri, M., Rayner, D., Lindberg, F., Thorsson, S., Knudby, A.J., Zickfeld, K., Middel, A., Krayenhoff, E.S., 2019. Urban tree planting to maintain outdoor thermal comfort under climate change: The case of Vancouver's local climate zones. Build. Environ. 158, 226–236. https://doi.org/10.1016/j.buildenv.2019.05.022.

Anderson, H., 2018. U.K. natural capital: Ecosystem accounts for urban areas. Office of National Statistics. Retrieved in May 2019 from: https://www.ons.gov.uk/releases/uknaturalcapitalecosystemaccountsforurbanareas.

Bagstad, K.J., Ancona, Z.H., Hass, J., Glynn, P.D., Wentland, S., Vardon, M., Fay, J., 2020. Integrating physical and economic data into experimental water accounts for the United States: Lessons and opportunities. Ecosyst. Serv. 45, 101182. https://doi.org/10.1016/j.ecoser.2020.101182.

Beatley, T., 2011. Biophilic cities: Integrating nature into urban design and planning. Island Press, Washington, DC.

Boyd, J.W., Bagstad, K.J., Ingram, J.C., Shapiro, C.D., Adkins, J.E., Casey, C.F., Duke, C. S., Glynn, P.D., Goldman, E., Grasso, M., Hass, J.L., Johnson, J.A., Lange, G.-M., Matuszak, J., Miller, A., Oleson, K.L.L., Posner, S.M., Rhodes, C., Soulard, F., … Wentland, S., 2018. The natural capital accounting opportunity: Let's really do the numbers. BioScience, 68(12), 940–943. https://doi.org/10.1093/biosci/biy135.

Bratman, G.N., Anderson, C.B., Berman, M.G., Cochran, B., de Vries, S., Flanders, J., Folke, C., Frumkin, H., Gross, J.J., Hartig, T., Kahn Jr., P.H., Kuo, M., Lawler, J.J., Levin, P.S., Lindahl, T., Meyer-Lindenberg, A., Mitchell, R., Ouyang, Z., Roe, J., Scarlett, L., Smith, J.R., van den Bosch, M., Wheeler, B.W., White, M.P., Zheng, H., Daily, G.C., 2019. Nature and mental health: an ecosystem service perspective. Sci. Adv. 5 (7), eaax0903. https://doi.org/10.1126/sciadv.aax0903.

Center for Urban Forest Research (2002). Fact Sheet #4: Control stormwater runoff with trees (p. 2). Retrieved from https://mostcenter.org/sites/default/files/resources/file/Trees%20for%20stormwater%20fact%20sheet.pdf. Accessed September 9, 2020.

City of Sacramento CA, 2019. Tree programs—City of Sacramento. Retrieved from https://www.cityofsacramento.org/Public-Works/Maintenance-Services/Trees/Programs. Accessed September 9, 2020.

City of Seattle, 2016. Tree canopy 2016 | City of Seattle Open Data portal. Retrieved from https://data.seattle.gov/Land-Base/Tree-Canopy-2016/w5tg-j5cp. Accessed September 9, 2020.

Cohen, D.T., Hatchard, G.W., Wilson, S., 2015. Population trends in incorporated places: 2000 to 2013. Retrieved from https://www.census.gov/content/dam/Census/library/publications/2015/demo/p25-1142.pdf. Accessed September 9, 2020.

Copernicus Global Land Service, 2020. Leaf Area Index: Version 1, 333m resolution, globe, 10-daily. Leaf Area Index. Retrieved from https://land.copernicus.vgt.vito.be/geonetwork/srv/eng/catalog.search#/metadata/urn:cgls:global:lai300_v1_333m. Accessed September 9, 2020.

Costhelper. (n.d.). How much does a rain garden cost? - CostHelper.com. CostHelper. Retrieved from https://home.costhelper.com/rain-garden.html. Accessed April 29, 2019.

Coulston, J.W., Moisen, G.G., Wilson, B.T., Finco, M.V., Cohen, W.B., Brewer, C.K., 2012. Modeling percent tree canopy cover: a pilot study. Photogramm. Eng. Remote Sens. 78 (7), 715–727. https://doi.org/10.14358/PERS.78.7.715.

Daly, Christopher, Halbleib, Michael, Smith, Joseph I., Gibson, Wayne P., Doggett, Matthew K., Taylor, George H., Curtis, Jan, Pasteris, Phillip P., 2008. Physiographically sensitive mapping of climatological temperature and precipitation across the conterminous United States. Int. J. Climatol. 28 (15), 2031–2064. https://doi.org/10.1002/joc.1688.

Declet-Barreto, J., Knowlton, K., Jenerette, G. D., Buyantuev, A., 2016. Effects of urban vegetation on mitigating exposure of vulnerable populations to excessive heat in Cleveland, Ohio. Weather, Climate, and Society, 8(4), 507–524. https://doi.org/10.1175/WCAS-D-15-0026.1.

Deilami, Kaveh, Kamruzzaman, Md., Liu, Yan, 2018. Urban heat island effect: a systematic review of spatio-temporal factors, data, methods, and mitigation measures. Int. J. Appl. Earth Obs. Geoinf. 67, 30–42. https://doi.org/10.1016/j.jag.2017.12.009.

Elmqvist, T., Setälä, H., Handel, S.N., van der Ploeg, S., Aronson, J., Blignaut, J.N., Gómez-Baggethun, E., Nowak, D.J., Kronenberg, J., de Groot, R., 2015. Benefits of restoring ecosystem services in urban areas. Curr. Opin. Enviro. Sustain. 14, 101–108. https://doi.org/10.1016/j.cosust.2015.05.001.

EO4EA, 2019. GEO Earth Observations for Ecosystem Accounting. EO4EA. Retrieved from https://www.eo4ea.org. Accessed September 9, 2020.

Erickson, A.J., Gulliver, J.S., Kang, J.-H., Weiss, P.T., Wilson, C.B., 2010. Maintenance for stormwater treatment practices. J. Contemporary Water Res. Educ. 146(1) 75–82. https://doi.org/10.1111/j.1936-704X.2010.00393.x.

Frost, J., 2017. Confidence intervals vs prediction intervals vs tolerance intervals. statistics by Jim. Retrieved from http://statisticsbyjim.com/hypothesis-testing/confidence-prediction-tolerance-intervals/. Accessed September 9, 2020.

Gillner, S., Vogt, J., Tharang, A., Dettmann, S., Roloff, A., 2015. Role of street trees in mitigating effects of heat and drought at highly sealed urban sites. Landscape Urban Plann. 143, 33–42. https://doi.org/10.1016/j.landurbplan.2015.06.005.

Greenfield, E., Nowak, D., Walton, J., 2009. Assessment of 2001 NLCD percent tree and impervious cover estimates. Photogramm. Eng. Remote Sens. 75 (11), 1279–1286. https://doi.org/10.14358/PERS.75.11.1279.

Grenier, M., Lantz, N., Soulard, F., Wang, J., 2020. The use of combined Landsat and Radarsat data for urban ecosystem accounting in Canada. Statistical Journal of the IAOS 36, 823–839. https://doi.org/10.3233/SJI-200663.

Hein, L., Bagstad, K., Edens, B., Obst, C., de Jong, R., Lesschen, J.P., 2016. Defining ecosystem assets for natural capital accounting. PLoS ONE 11 (11), e0164460. https://doi.org/10.1371/journal.pone.0164460.

Heris, M., Troy, A., 2018. Denver Open Data Catalog: Tree Canopy (2014). Retrieved from https://www.denvergov.org/opendata/dataset/tree-canopy-2014. Accessed September 9, 2020.

Heris, M.P., Middel, A., Muller, B., 2020a. Impacts of form and design policies on urban microclimate: assessment of zoning and design guideline choices in urban redevelopment projects. Landscape Urban Plann. 202, 103870 https://doi.org/10.1016/j.landurbplan.2020.103870.

Heris, M.P., Foks, N.L., Bagstad, K.J., Troy, A., Ancona, Z., 2020b. A rasterized building footprint dataset for the United States. Sci. Data 7 (1), 1–10. https://doi.org/10.1038/s41597-020-0542-3.

Hirabayashi, S., 2013. I-Tree Eco precipitation interception model descriptions. Retrieved from https://www.itreetools.org/documents/61/iTree_Eco_Precipitation_Interception_Model_Descriptions.pdf. Accessed September 9, 2020.

Keeler, B.L., Hamel, P., McPhearson, T., Hamann, M.H., Donahue, M.L., Meza Prado, K. A., Arkema, K.K., Bratman, G.N., Brauman, K.A., Finlay, J.C., Guerry, A.D., Hobbie, S.E., Johnson, J.A., MacDonald, G.K., McDonald, R.I., Neverisky, N., Wood, S.A., 2019. Social-ecological and technological factors moderate the value of urban nature. Nat. Sustainability 2 (1), 29–38. https://doi.org/10.1038/s41893-018-0202-1.

Klaassen, W., Bosveld, F., de Water, E., 1998. Water storage and evaporation as constituents of rainfall interception. J. Hydrol. 212–213, 36–50. https://doi.org/10.1016/S0022-1694(98)00200-5.

Klingberg, J., Broberg, M., Strandberg, B., Thorsson, P., Pleijel, H., 2017. Influence of urban vegetation on air pollution and noise exposure – a case study in Gothenburg, Sweden. Sci. Total Environ. 599–600, 1728–1739. https://doi.org/10.1016/j.scitotenv.2017.05.051.

Kong, F., Sun, C., Liu, F., Yin, H., Jiang, F., Pu, Y., Cavan, G., Skelhorn, C., Middel, A., Dronova, I., 2016. Energy saving potential of fragmented green spaces due to their temperature regulating ecosystem services in the summer. Appl. Energy 183, 1428–1440. https://doi.org/10.1016/j.apenergy.2016.09.070.

Livesley, S.J., McPherson, E.G., Calfapietra, C., 2016. The urban forest and ecosystem services: impacts on urban water, heat, and pollution cycles at the tree, street, and city scale. J. Environ. Qual. 45 (1), 119–124. https://doi.org/10.2134/jeq2015.11.0567.

Mackey, C., Galanos, T., Norford, L., Roudsari, M.S., 2017. Wind, sun, surface temperature, and heat island: Critical variables for high-resolution outdoor thermal comfort. Proceedings of the 15th International Conference of Building Performance Simulation Association. San Francisco, USA. Retrieved from https://www.ladybug.tools/assets/pdf/BS2017_260.pdf. Accessed September 9, 2020.

McDonald, R.I., Kroeger, T., Zhang, P., Hamel, P., 2020. The Value of U.S. urban tree cover for reducing heat-related health impacts and electricity consumption. Ecosystems 23 (1), 137–150. https://doi.org/10.1007/s10021-019-00395-5.

McPhearson, T., Andersson, E., Elmqvist, T., Frantzeskaki, N., 2015. Resilience of and through urban ecosystem services. Ecosyst. Serv. 12, 152–156. https://doi.org/10.1016/j.ecoser.2014.07.012.

McPherson, E.G., Simpson, J.R., Xiao, Q., Wu, C., 2011. Million trees Los Angeles canopy cover and benefit assessment. Landscape Urban Plann. 99 (1), 40–50. https://doi.org/10.1016/j.landurbplan.2010.08.011.

Meier, G.A., Brown, J.F., 2014. Remote sensing of land surface phenology. U.S. Geological Survey Fact Sheet 2014-3052, 2 p. Retrieved from https://pubs.er.usgs.gov/publication/fs20143052. Accessed September 9, 2020.

Menne, M.J., Durre, I., Vose, R.S., Gleason, B.E., Houston, T.G., 2012. An overview of the global historical climatology network-daily database. J. Atmos. Oceanic Technol. 29 (7), 897–910. https://doi.org/10.1175/JTECH-D-11-00103.1.

Microsoft, 2018. United States building footprints. Retrieved from https://github.com/Microsoft/USBuildingFootprints. Accessed December 14, 2018.

Middel, A., Chhetri, N., Quay, R., 2015. Urban forestry and cool roofs: assessment of heat mitigation strategies in Phoenix residential neighborhoods. Urban For. Urban Greening 14 (1), 178–186. https://doi.org/10.1016/j.ufug.2014.09.010.

Middel, A., Krayenhoff, E.S., 2019. Micrometeorological determinants of pedestrian thermal exposure during record-breaking heat in Tempe, Arizona: introducing the MaRTy observational platform. Sci. Total Environ. 687, 137–151. https://doi.org/10.1016/j.scitotenv.2019.06.085.

Mullaney, J., Lucke, T., Trueman, S.J., 2015. A review of benefits and challenges in growing street trees in paved urban environments. Landscape Urban Plann. 134, 157–166. https://doi.org/10.1016/j.landurbplan.2014.10.013.

Narayanan, A., Pitt, R., 2002. Costs of urban stormwater control practices (EPA Report). Department of Civil and Environmental Engineering, The University of Alabama. Retrieved from http://rpitt.eng.ua.edu/class/International%20urban%20water%20systems/Arvind%20Costs%20of%20Urban%20Stormwater%20Control%20Feb%2005%202006%20clean%20copy.htm. Accessed September 9, 2020.

National Centers for Environmental Information, 2018. Global Historical Climatology Network—Daily (GHCN-Daily), Version 3. Retrieved from https://data.nodc.noaa.gov/cgi-bin/iso?id=gov.noaa.ncdc:C00861. Accessed September 9, 2020.

New York City, 2017. Land Cover Raster Data (2017) – 6 Inch Resolution | NYC Open Data. Retrieved from https://data.cityofnewyork.us/Environment/Land-Cover-Raster-Data-2017-6in-Resolution/he6d-2qns. Accessed September 9, 2020.

Norwegian Institute for nature research (NINA), 2019. Urban Experimental Ecosystem Accounting website. Retrieved from http://urban.nina.no/. Accessed May 9, 2019.

Nowak, D.J., Appleton, N., Ellis, A., Greenfield, E., 2017. Residential building energy conservation and avoided power plant emissions by urban and community trees in the United States. Urban For. Urban Greening 21, 158–165. https://doi.org/10.1016/J.UFUG.2016.12.004.

Nowak, D.J., Bodine, A.R., Hoehn, R.E.I., Crane, D.E., Ellis, A., Endreny, T.A., Yang, Y., Jacobs, T., Shelton, Kassie, 2013. Assessing urban forest effects and values: The greater Kansas City region (NRS-RB-75; p. NRS-RB-75). U.S. Department of Agriculture, Forest Service, Northern Research Station. https://doi.org/10.2737/NRS-RB-75.

Nowak, D.J., Crane, D.E., Stevens, J.C., 2006. Air pollution removal by urban trees and shrubs in the United States. Urban For. Urban Greening 4 (3), 115–123. https://doi.org/10.1016/j.ufug.2006.01.007.

Nowak, D.J., Dwyer, J.F., 2007. Understanding the benefits and costs of urban forest ecosystems. In: Kuser, J.E. (Ed.), Urban and Community Forestry in the Northeast. Springer, Netherlands, Dordrecht, pp. 25–46. https://doi.org/10.1007/978-1-4020-4289-8_2.

Nowak, D.J., Greenfield, E.J., 2012. Tree and impervious cover in the United States. Landscape Urban Plan. 107, 21–30. https://doi.org/10.1016/j.landurbplan.2012.04.005.

Nowak, D.J., Greenfield, E.J., 2018. Declining urban and community tree cover in the United States. Urban For. Urban Greening 32, 32–55. https://doi.org/10.1016/j.ufug.2018.03.006.

Nowak, D.J., Hirabayashi, S., Bodine, A., Greenfield, E., 2014. Tree and forest effects on air quality and human health in the United States. Environ. Pollut. 193, 119–129. https://doi.org/10.1016/j.envpol.2014.05.028.

Obst, C., Hein, L., Edens, B., 2016. National accounting and the valuation of ecosystem assets and their services. Environ. Resour. Econ. 64 (1), 1–23. https://doi.org/10.1007/s10640-015-9921-1.

Oke, T.R., 1989. The micrometeorology of the urban forest. Philos. Trans. R. Soc. London B, Biol. Sci. 324 (1223), 335–349. https://doi.org/10.1098/rstb.1989.0051.

Riley, C.B., Gardiner, M., 2020. Examining the distributional equity of urban tree canopy cover and ecosystem services across United States cities. PLoS ONE 15 (2), e0228499. https://doi.org/10.1371/journal.pone.0228499.

Santamouris, M., Cartalis, C., Synnefa, A., Kolokotsa, D., 2015. On the impact of urban heat island and global warming on the power demand and electricity consumption of buildings—a review. Energy Build. 98, 119–124. https://doi.org/10.1016/j.enbuild.2014.09.052.

Scurlock, J.M.O., Asner, G.P., Gower, S.T., 2001. Global leaf area index from field measurements, 1932–2000. ORNL DAAC. https://doi.org/10.3334/ORNLDAAC/584.

Shashua-Bar, L., Hoffman, M.E., 2000. Vegetation as a climatic component in the design of an urban street: An empirical model for predicting the cooling effect of urban green areas with trees. Energy Build. 31 (3), 221–235. https://doi.org/10.1016/S0378-7788(99)00018-3.

Statistics Canada. 2016. Human Activity and the Environment 2015: The Changing landscape of Canadian metropolitan areas. Catalogue no. 16–201-X. Retrieved from https://www150.statcan.gc.ca/n1/en/pub/16-201-x/16-201-x2016000-eng.pdf?st=Dm16ncqD/. Accessed December 13, 2020.

Steele, M.K., Wolz, H., 2019. Heterogeneity in the land cover composition and configuration of US cities: implications for ecosystem services. Landscape Ecol. 34 (6), 1247–1261. https://doi.org/10.1007/s10980-019-00859-y.

Stovin, V.R., Jorgensen, A., Clayden, A., 2008. Street trees and stormwater management. Arboricul. J. 30 (4), 297–310. https://doi.org/10.1080/03071375.2008.9747509.

Tan, Z., Lau, K.K.-L., Ng, E., 2016. Urban tree design approaches for mitigating daytime urban heat island effects in a high-density urban environment. Energy Build. 114, 265–274. https://doi.org/10.1016/j.enbuild.2015.06.031.

Tavares, P.A., Beltrão, N., Guimarães, U.S., Teodoro, A., Gonçalves, P., 2019. Urban ecosystem services quantification through remote sensing approach: a systematic review. Environments 6 (5), 51. https://doi.org/10.3390/environments6050051.

Taylor, J.R., 1997. An introduction to error analysis: The study of uncertainties in physical measurements. University Science Books, Sausalito, CA.

Theobald, D.M., 2014. Development and applications of a comprehensive land use classification and map for the US. PLoS ONE 9 (4). https://doi.org/10.1371/journal.pone.0094628.

United Nations, 2015. Sustainable development goals: The 17 goals. Department of Economic and Social Affairs website. Retrieved from https://sdgs.un.org/goals. Accessed May 13, 2020.

United Nations, 2017. SEEA experimental ecosystem accounting: Technical recommendations. Retrieved from https://seea.un.org/sites/seea.un.org/files/technical_recommendations_in_support_of_the_seea_eea_final_white_cover.pdf. Accessed May 13, 2020.

United Nations et al., 2014a. System of environmental-economic accounting 2012: Central framework. Retrieved from https://seea.un.org/sites/seea.un.org/files/seea_cf_final_en.pdf. Accessed May 13, 2020.

United Nations et al., 2014b. System of environmental-economic accounting 2012: Experimental ecosystem accounting. Retrieved from https://seea.un.org/sites/seea.un.org/files/seea_eea_final_en_1.pdf. Accessed May 13, 2020.

United Nations et al., 2020. SEEA experimental ecosystem accounting revision 2020: Revision issues note – Final. Retrieved from https://seea.un.org/sites/seea.un.org/files/documents/EEA/2_seea_eea_rev._ch5_gc_mar2020_final.pdf. Accessed May 13, 2020.

U.S. Census Bureau, 2019. TIGER/Line Shapefiles. Retrieved from https://www.census.gov/geographies/mapping-files/time-series/geo/tiger-line-file.html. Accessed May 19, 2019.

U.S. Department of Agriculture and Davey Tree, 2020. i-Tree Hydro Software. Retrieved from https://www.itreetools.org/tools/hydro. Accessed May 13, 2020.

U.S. Department of Energy, 2019. Building Performance Database. Retrieved from https://www.energy.gov/eere/buildings/building-performance-database-bpd#:~:text=Project%20Overview,of%20commercial%20and%20residential%20buildings.&text=Information%20about%20the%20BPD%20API,on%20the%20BPD%20developers%20page. Accessed May 13, 2019.

U.S. Energy Information Administration, 2019. State energy portal featuring customizable dashboards and more state data. Retrieved from https://www.eia.gov/state/. Accessed June 12, 2019.

U.S. Environmental Protection Agency, (2014). Heat island impacts [Overviews and Factsheets]. Retrieved from https://www.epa.gov/heat-islands/heat-island-impacts. Accessed May 13, 2019.

U.S. Environmental Protection Agency, 2020. Enforcement and compliance history online [Data & Tools]. Enforcement and Compliance History Online. Retrieved from https://echo.epa.gov/. Accessed September 9, 2020.

U.S. Geological Survey. (2017). USGS water resources: Hydrologic unit maps. Retrieved from https://water.usgs.gov/GIS/huc.html. Accessed September 9, 2020.

U.S. Geological Survey, 2019. Landsat 8 (L8) data users handbook: Version 5.0. In Landsat Missions. Retrieved from https://prd-wret.s3.us-west-2.amazonaws.com/assets/palladium/production/atoms/files/LSDS-1574_L8_Data_Users_Handbook-v5.0.pdf. Accessed September 9, 2020.

U.S. Geological Survey (2020). Accounting for natural capital. Retrieved from https://www.usgs.gov/centers/gecsc/science/accounting-natural-capital-building-numbers-track-and-sustain-nation-s-natural?qt-science_center_objects=0#qt-science_center_objects. Accessed May 13, 2020.

U. S. Office of Management and Budget, 2017. The North American Industry Classification System (NAICS). In Dictionary of Marketing Communications. https://doi.org/10.4135/9781452229669.n2410.

Wang, J., Endreny, T.A., Nowak, D.J., 2008. Mechanistic simulation of tree effects in an urban water balance model. JAWRA J. Am. Water Resour. Assoc. 44 (1), 75–85. https://doi.org/10.1111/j.1752-1688.2007.00139.x.

Warnell, K.J.D., Russell, M., Rhodes, C., Bagstad, K.J., Olander, L.P., Nowak, D.J., Poudel, R., Glynn, P.D., Hass, J.L., Hirabayashi, S., Ingram, J.C., Matuszak, J., Oleson, K.L.L., Posner, S.M., Villa, F., 2020. Testing ecosystem accounting in the United States: a case study for the Southeast. Ecosyst. Serv. 43, 101099 https://doi.org/10.1016/j.ecoser.2020.101099.

Wentland, S.A., Ancona, Z.H., Bagstad, K.J., Boyd, J., Hass, J.L., Gindelsky, M., Moulton, J.G., 2020. Accounting for land in the United States: Integrating physical land cover, land use, and monetary valuation. Ecosystem Services 46, 101178. https://doi.org/10.1016/j.ecoser.2020.101178.

Wickham, J., Stehman, S.V., Neale, A.C., Mehaffey, M., 2020. Accuracy assessment of NLCD 2011 percent impervious cover for selected USA metropolitan areas. Int. J. Appl. Earth Obs. Geoinf. 84, 101955 https://doi.org/10.1016/j.jag.2019.101955.

Willcock, S., Martínez-López, J., Hooftman, D.A.P., Bagstad, K.J., Balbi, S., Marzo, A., Prato, C., Sciandrello, S., Signorello, G., Voigt, B., Villa, F., Bullock, J.M., Athanasiadis, I.N., 2018. Machine learning for ecosystem services. Ecosyst. Serv. 33, 165–174. https://doi.org/10.1016/j.ecoser.2018.04.004.

Willis, K.J., Petrokofsky, G., 2017. The natural capital of city trees. Science 356 (6336), 374–376. https://doi.org/10.1126/science.aam9724.

Wolch, J.R., Byrne, J., Newell, J.P., 2014. Urban green space, public health, and environmental justice: The challenge of making cities 'just green enough'. Landscape Urban Plann. 125, 234–244. https://doi.org/10.1016/j.landurbplan.2014.01.017.

Xiao, Q., McPherson, E.G., 2002. Rainfall interception by Santa Monica's municipal urban forest. Urban Ecosyst. 6 (4), 291–302. https://doi.org/10.1023/B:UECO.0000004828.05143.67.

Xiao, Q., McPherson, E.G., Simpson, J.R., Ustin, S.L., 1998. Rainfall interception by Sacramento's urban forest. J. Arboric. 24, 235–244.

Xiao, Q., McPherson, E.G., Ustin, S.L., Grismer, M.E., 2000. A new approach to modeling tree rainfall interception. J. Geophys. Res.: Atmos. 105 (D23), 29173–29188. https://doi.org/10.1029/2000JD900343.

Yang, L., Jin, S., Danielson, P., Homer, C., Gass, L., Bender, S.M., Case, A., Costello, C., Dewitz, J., Fry, J., Funk, M., Granneman, B., Liknes, G.C., Rigge, M., Xian, G., 2018. A new generation of the United States National Land Cover Database: requirements, research priorities, design, and implementation strategies. ISPRS J. Photogramm. Remote Sens. 146 (September), 108–123. https://doi.org/10.1016/j.isprsjprs.2018.09.006.

Zhou, W., Wang, J., Cadenasso, M.L., 2017. Effects of the spatial configuration of trees on urban heat mitigation: a comparative study. Remote Sens. Environ. 195, 1–12. https://doi.org/10.1016/j.rse.2017.03.043.

Ziter, C.D., Pedersen, E.J., Kucharik, C.J., Turner, M.G., 2019. Scale-dependent interactions between tree canopy cover and impervious surfaces reduce daytime urban heat during summer. Proc. Natl. Acad. Sci. 116 (15), 7575–7580. https://doi.org/10.1073/pnas.1817561116.